THE MECHANICAL PROPERTIES OF MULTI-YEAR SEA ICE, PHASE II: ICE STRUCTURE ANALYSIS

J.A. Richter-Menge and
N. M. Perron

U.S. Army Cold Regions Research
and Engineering Laboratory
72 Lyme Road
Hanover, NH 03755-1290

THE MECHANICAL PROPERTIES OF MULTI-YEAR SEA ICE
PHASE II: ICE STRUCTURE ANALYSIS

by

Jacqueline A. Richter-Menge and Nancy M. Perron

This report presents the ice structure analysis of multi-year pressure ridge ice samples tested in the second phase of a joint government-industry study. The study was initiated to systematically examine the structure and mechanical properties of ice samples taken from multi-year ridges. Interest in the properties of multi-year ridges stems from the fact that these ridges are the most frequently encountered, massive ice features in exposed areas of the Beaufort and Chukchi Seas. Deep water oil platforms constructed in this area of the arctic must be designed, therefore, to withstand the impact of a multi-year ridge.

Both Phase I and II of this program involved field sampling in the southern Beaufort Sea. The field program for Phase I was conducted in April 1981 and involved the sampling of 10 different pressure ridges. A continuous, vertical multi-year ridge core was also specifically obtained for detailed structural analysis. A total of 220 unconfined uniaxial constant-strain-rate compression tests were done on the vertically cored ice samples from the 10 ridges. The preliminary ice structure analysis of these test specimens indicated that the main factor contributing to large variations in the test results was associated with the extreme local variability of ice structure within a ridge. It became apparent that a complete and useful analysis of the multi-year ridge ice property test data would require a thorough structural interpretation of each test sample.

Additional multi-year ice from 4 ridges was collected in April 1982 for the Phase II tests. Included in these field samples were horizontally and vertically cored ice samples taken in close proximity to another. These matched pairs were tested in unconfined, uniaxial constant-strain-rate compression to investigate the effect of sample orientation on the test results. The remaining vertical ice samples were used in additional unconfined compression tests and in confined constant-strain-rate compression, constant-strain-rate tension, and constant load compression tests. A total of 188 tests were done in Phase II. During the Phase II field program, we also took a second vertically drilled continuous ridge core to augment the ice structure data obtained in Phase I.

This report includes the ice structure analyis of the Phase II multi-year pressure ridge test specimens with the exception of the constant load compression tests. We have also included the analysis of the continuous ridge core taken during the second field program. The structural analysis of the ice samples tested in Phase I is presented in Richter-Menge et al. (in prep, a). Discussions on the field sampling program and the test results and analyses for Phases I and II can be found in Cox et al. (1984, 1985), respectively.

SAMPLE ANALYSIS

The structural characteristics of the continous multi-year ridge core and the Phase II ridge test specimens were evaluated using the same techniques described in Richter-Menge et al. (in prep, a). Briefly, ice thin sections were prepared from the sample after testing. If a sample was destroyed during the test, end pieces taken immediately adjacent to the test specimen were used to interpret the structural composition of the

sample. The ice type was determined by studying the photographs of the thin sections between cross polarizers.

The ice type of each sample was described according to the multi-year pressure ridge ice structural classification scheme summarized in Table 1. Figure 1 shows a series of thin sections, photographed between crossed polarizers, that illustrates the principal structural characteristics of each ice type. This structural classification scheme divides the ice into three major ice texture categories; granular, columnar, or a mixture of columnar and granular ice. If a sample was classified as columnar, or contained large fragments of columnar ice, the ice thin sections were analyzed on the universal stage. Using these measurements we defined the mean angle between the crystallographic c-axes and the load direction (σ:c) and the degree of alignment of the c-axes (° spread). We also used the thin section analysis to determine the angle between the columns, or direction of elongation of the crystals, and the load (σ:z). The photographed thin sections of each sample helped to confirm these measurements. Note that all of our samples, both horizontally and vertically cored, were cylindrical. The compressive or tensile load was applied along the cylindrical axis of the samples. For vertically cored samples then, σ:z also represents the angle between the direction of elongation and the vertical. Thin sections taken perpendicular to the load were used for the crystallographic measurements to avoid misinterpretation as a result of apparent dip and plunge.

The granular ice in the thin sections was not analyzed on the universal stage because the grain size was too small, averaging 1 mm in diameter.

Table 1. Structural classification scheme for multi-year pressure ridge ice samples.

Ice Type	Code	Structural Characteristics
Granular	I	Isotropic, equiaxed crystals
Columnar	II	Elongated, columnar grains
	IIA	Columnar sea ice with c-axes normal to growth direction; axes may or may not be aligned
	IIC	Columnar freshwater ice
Mixed	III	Combination of Types I and III
	IIIA	Largely Type II with granular veins
	IIIB	Largely Type I with inclusions of Type I or II ice (brecciated ice)

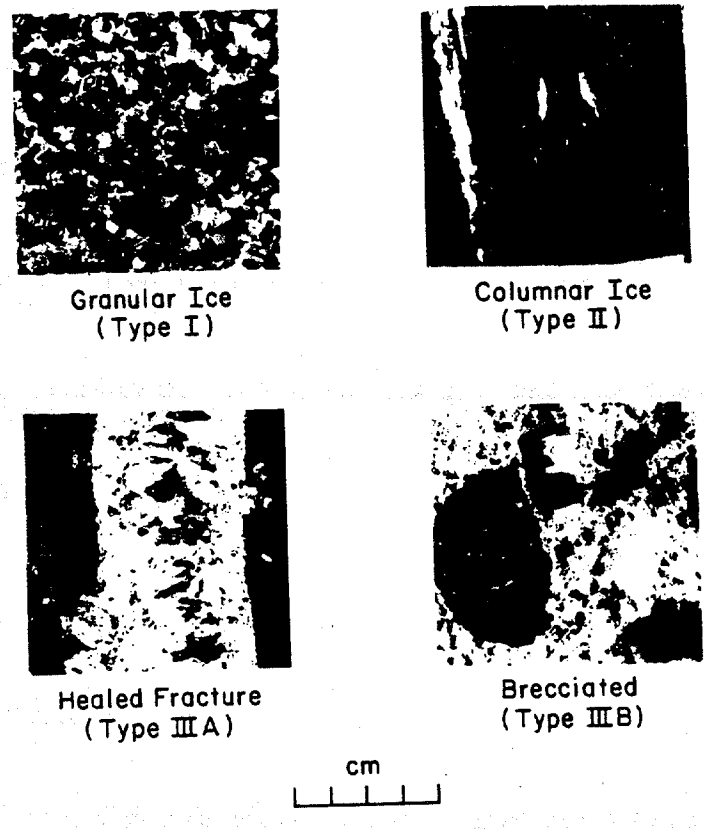

Figure 1. Structural characteristics of multi-year ice types.

ROUTING AND TRANSMITTAL SLIP

Date 17 Oct

TO: (Name, office symbol, room number, building, Agency/Post)	Initials	Date
1. Charlie		
2.		
3.		
4.		
5.		

Action	File	Note and Return
Approval	For Clearance	Per Conversation
As Requested	For Correction	Prepare Reply
Circulate	For Your Information	See Me
Comment	Investigate	Signature
Coordination	Justify	

REMARKS

I just discovered that page 11 is missing from the Phase II structure report. Here is a copy of that elusive page for incorporation into your copy of the draft report.

Mike.

DO NOT use this form as a RECORD of approvals, concurrences, disposals, clearances, and similar actions

FROM: (Name, org. symbol, Agency/Post) | Room No.—Bldg. | Phone No.

OPTIONAL FORM 41 (Rev. 7-76)
Prescribed by GSA
FPMR (41 CFR) 101-11.206

5041-102
☆U.S. G.P.O. 1983-414-517

5 and -20°C, 10^{-2} s^{-1}

ease in strength

a leveling off in

-Menge et al. (in

n transversely

Unfortunately,

urally analyzed

ests. The ice

itions. Thin

he test specimen

e cold-storage

n-rate compres-

ase I (Mellor

radial confin-

g applied; $\sigma_1 >$

ion tests were

$^{-3}$ and 10^{-5}

and the

z, respectively. A total of 55 confined compression tests were completed. Plots of strength versus porosity that include the structural classification and crystallographic measurements of the tested ice samples are given in Figures 6a-f. In Table 4, we have summarized the percent granular, columnar and mixed ice samples at each test condition.

The granular ice was observed between crossed polarizers and the crystals appeared to be randomly oriented.

The maximum, minimum and mean grain sizes of the columnar and/or granular crystals in each sample were estimated by using the thin section photographs. Each photograph contained a millimeter scale next to the thin section for grain size analysis. The grain size measurements in the tension tests were made at the location of the failure plane. Unlike the compression tests, the tension samples all failed via an extension mechanism. The failure plane was normal to the load and easily identified in the thin section photographs. For the compression test specimens, we based our grain size measurements on the textural characteristics of the entire sample.

Backlighting was again used to determine the gross structural features of the ice samples. Photographs of the sample at noted positions were taken before and after the test. The two sets of photographs were compared to distinguish between original and test-created ice textures in the unconfined and confined compression tests where the ice underwent considerable deformation. The post-test photographs of the sample were also used to determine the mode and location of the failure. The type of failure was described using Figure 2, taken from Jaeger and Cook (1969).

The Phase II continuous multi-year pressure ridge core was indexed with a vertical line along its entire length before thin sectioning. The core was thin cut into 10 cm segments and thin sectioned. A continuous structural profile of this core was prepared from the photographs taken of these thin sections between crossed polarizers. This structural profile is

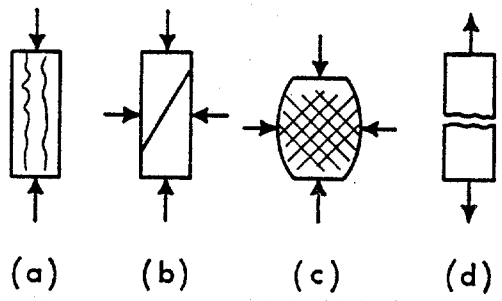

Figure 2. Typical failure modes; in compression, (a) longitudinal splitting, (b) shear fracture, and (c) multiple shear fractures and, in tension, (d) extension fracture.

presented in Cox et al. (1985) together with a detailed description of the ice structure.

CONTINUOUS MULTI-YEAR RIDGE CORE

A schematic structural profile of the Phase II continuous vertical multi-year pressure ridge core is presented in Figure 3. Well-defined columnar zones in the core, indicated by the letter C, include a measurement of the angle between the direction of elongation of the crystals and the vertical (σ:z). We also note whether the crystal c-axes in the columnar ice were aligned or unaligned.

Nearly 50% of the ice in the Phase II core is columnar. The zones of columnar ice are distributed throughout the core, unlike the Phase I continuous core in which most of the columnar ice was concentrated at the bottom of the core. The remainder of the Phase II core is a combination of granular ice and mixed granular and columnar crystals. The mixed ice is predominately brecciated, composed of columnar fragments in a granular matrix. Based on these characteristics, it would appear that this multi-year ridge (Ridge C) was initially formed by the compression of two adjacent ice sheets. We would anticipate a much lower percentage of columnar ice in a ridge formed by shearing.

As observed in the Phase I continuous ridge core and many of the Phase I test samples, the angle between the vertical and the direction of elongation of the crystals in the columnar zones of the Phase II core is 15° or less. There is only one exception, at 350 cm one section of columnar ice has a σ:z angle of 35°. This indicates that in Ridge C, the columnar blocks were lying in a near-horizontal position.

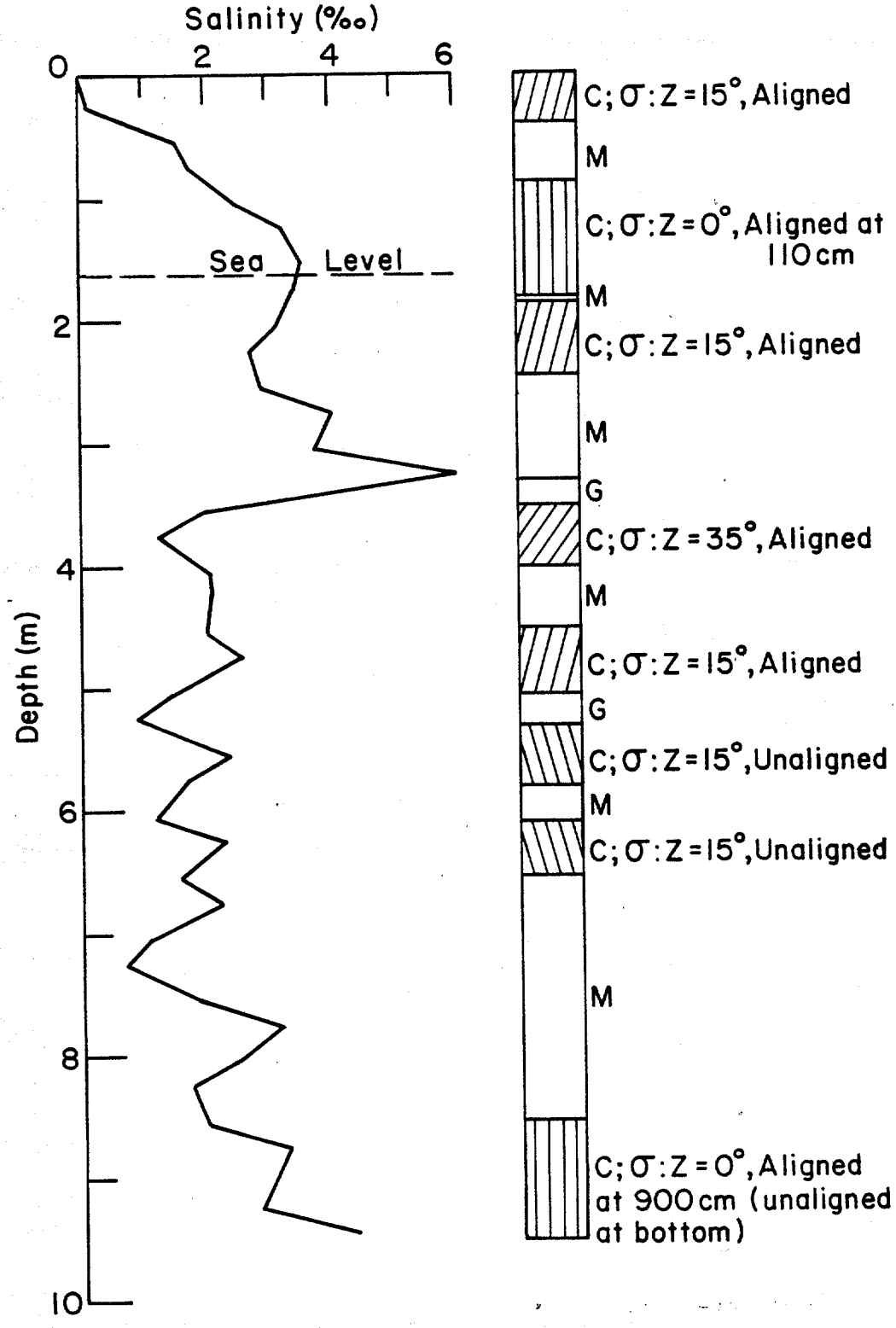

Figure 3. Salinity and schematic structural profile for the Phase II continuous multi-year pressure ridge core. G = granular ice, C = columnar ice, M = mixed granular and columnar ice.

TESTED MULTI-YEAR RIDGE ICE SAMPLES

In this section we present the results of the ice structure analysis of the Phase II multi-year ridge test specimens. Phase I results are included whenever it is appropriate. This additional data has helped us in the interpretation of the effect of ice structure on the Phase II test results. The structural classification and crystallographic measurements made on each Phase II test specimen are given in Appendix A. The samples are grouped according to test condition. The fracture mode for the tension tests is not listed in these tables since all of the samples failed via an extension mechanism (Fig. 2d). In Table 2, we have listed the total number of Phase II samples tested in each major loading state, noting the ridges that the samples were taken from and the number of columnar samples in each group.

Unconfined constant-strain-rate compression tests

The Phase II unconfined, uniaxial constant-strain-rate compression tests were done at two temperatures (-5 and -20°C) and two strain-rates (10^{-2} and 10^{-4} s^{-1}). The test parameters were chosen to compliment the unconfined constant-strain-rate compression tests done in Phase I at the same temperature, but at strain rates of 10^{-3} and 10^{-5} s^{-1}. Matched pairs of horizontally and vertically cored samples were tested at -5 and -20°C and a strain rate of 10^{-4} s^{-1} to determine the effect of sample orientation on the compressive strength of the multi-year ice. These samples were paired according to their location within the ridge. We have summarized the percent granular, columnar and mixed ice samples at each test condition in Phase I and II in Table 3. As noted in the Phase I ice structure analysis report, the most common ice type by far is the mixed columnar and

Table 2. Columnar ice samples tested in Phase II. These samples include both columnar and mixed samples with greater than or equal to 80% columnar ice.

Test Type	Ridge No.	Total number of samples tested	Total number of columnar samples	% Columnar samples
Unconfined Compression	A	9	0	0
	C	53	20	38
Confined Compression	A	22	0	0
	B	33	7	21
Tension	A	15	1	7
	B	21	2	10
Total		153	30	20

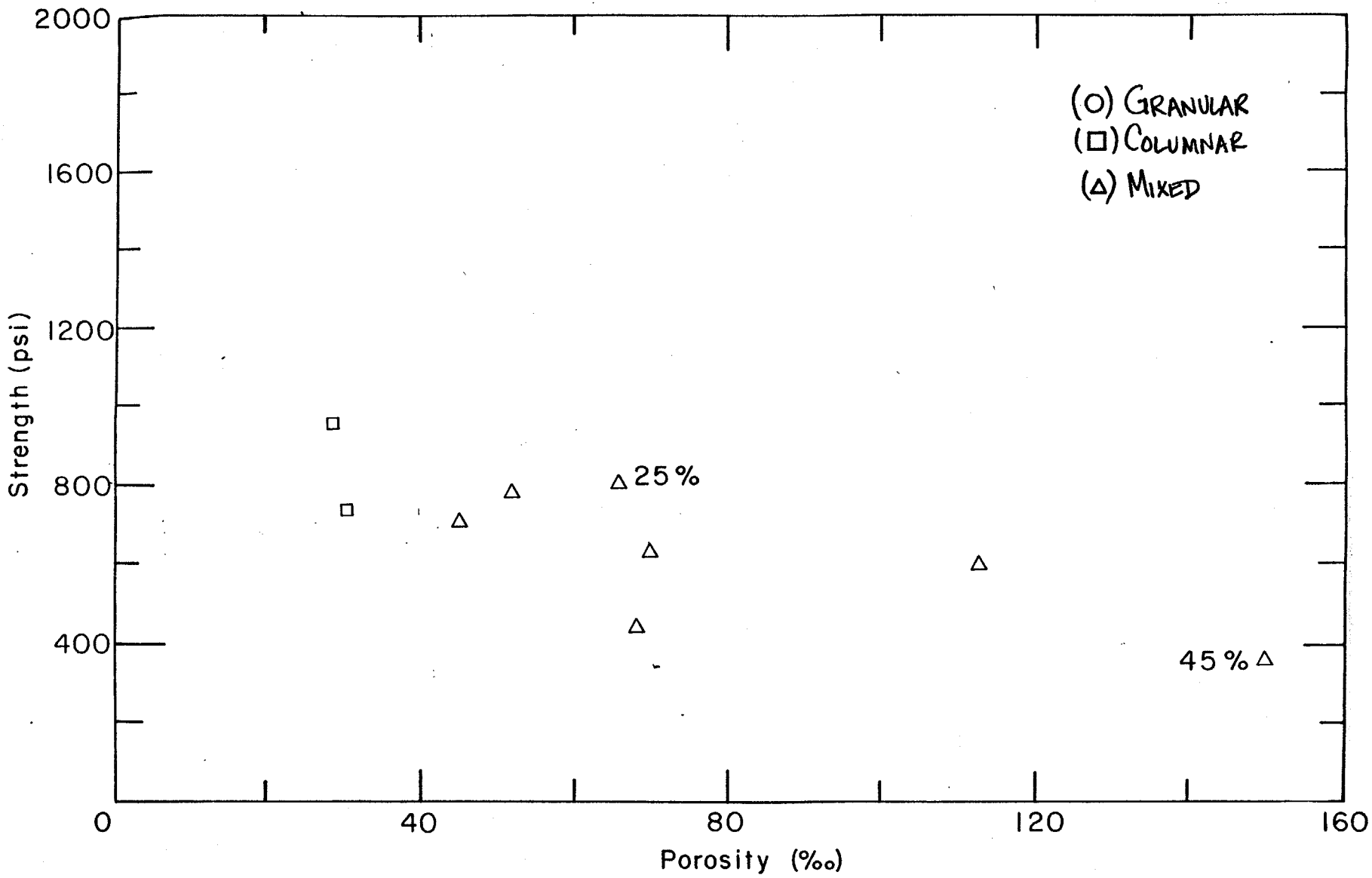

a. Tests conducted at 10^{-2} s^{-1} and -5°C.

Figure 4. Unconfined, constant-strain-rate compressive strength versus porosity for all Phase II ridge ice samples with the structural classification indicated for each sample. Open symbols = vertically cored samples and closed symbols = horizontally cored samples. Crystallographic measurements indicated next to each sample: (σ:z, σ:c), % columnar, °spread.

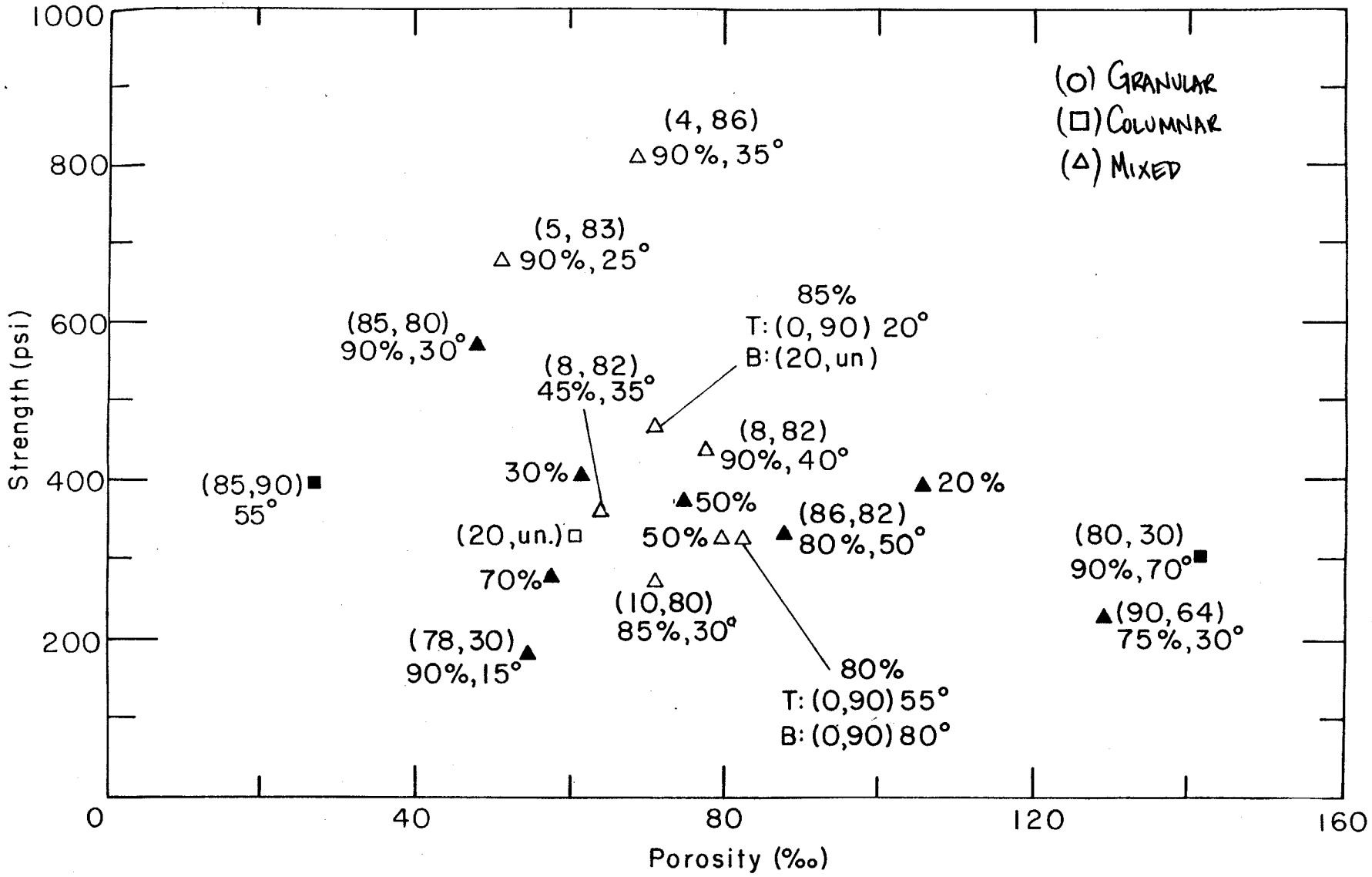

b. Tests conducted at 10^{-4} s^{-1} and -5°C.

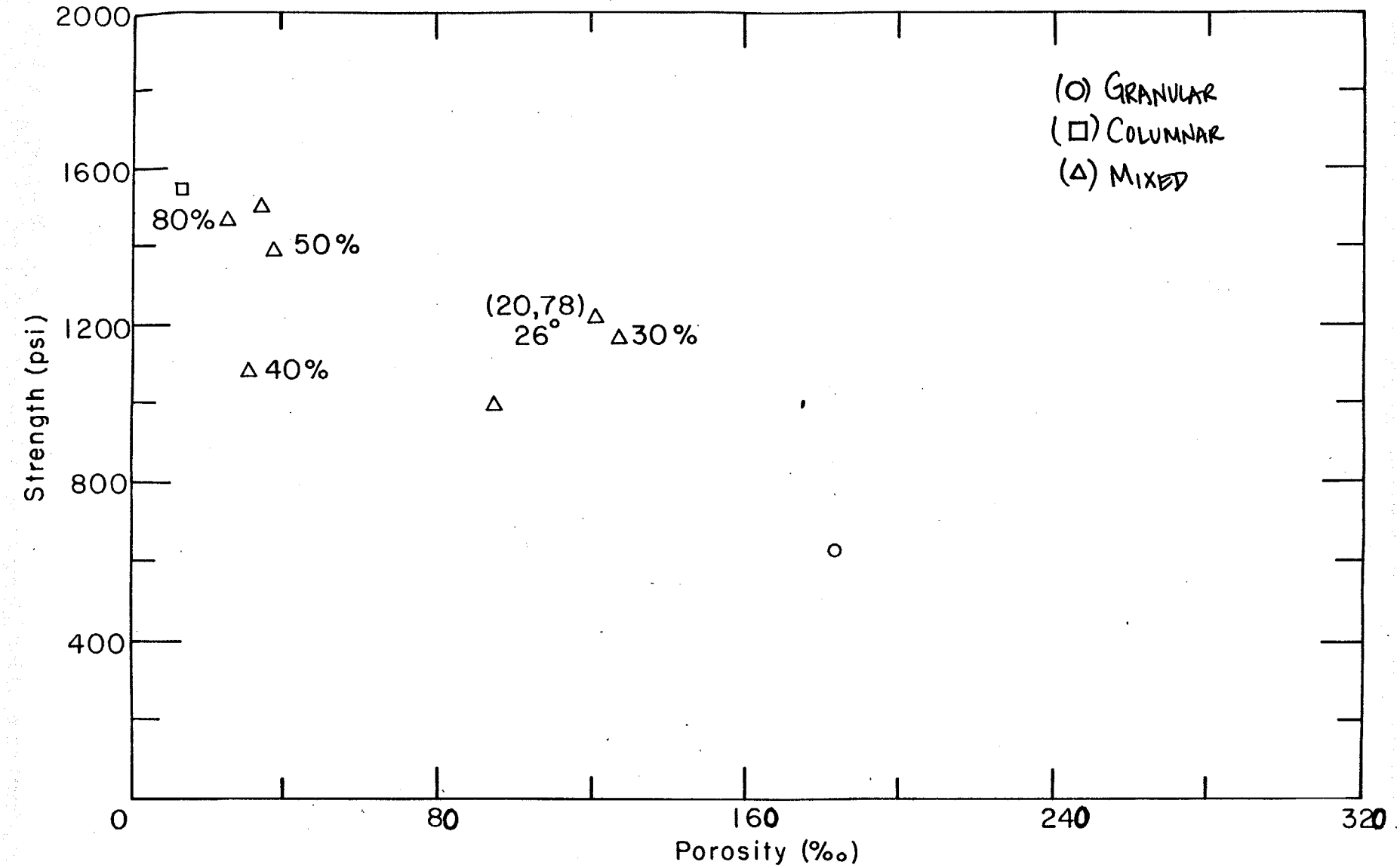

c. Tests conducted at 10^{-2} s^{-1} and -20°C.

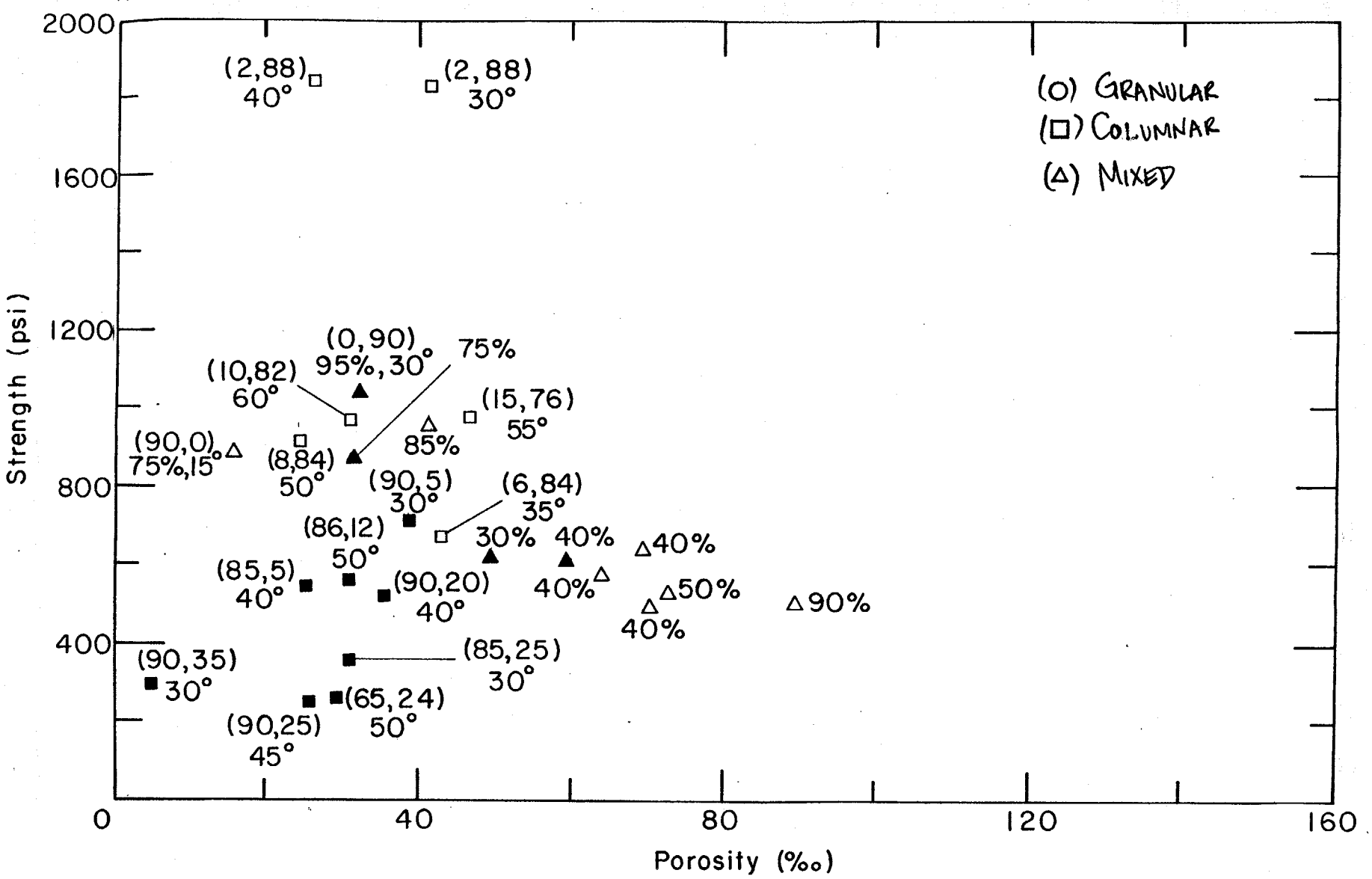

d. Tests conducted at 10^{-4} s^{-1} and -20°C.

of the strength versus porosity band. At all test conditions, 10^{-4} and 10^{-2} s^{-1}, there is a tendency for the compressive strength of the mixed and granular ice samples to decrease with an increase in porosity. The influence of grain size on the compressive strength of the ridge samples appears insignificant compared to the effects of crystal orientation and porosity.

All of the matched sample pairs we tested were obtained from Ridge C, the same ridge that provided the continuous ridge core described in the previous section. The tests done on the matched pairs (Fig. 4b and d) do indicate that the mean compressive strength of ice samples from a multi-year ridge is dependent on sample orientation. Vertically cored samples tend to give a higher mean strength than horizontally cored samples. The dependency of mean compressive strength on sample orientation can be explained by sample ice structure. The ice structure analysis of the ridges we have samples, including Ridge C, suggests that most of the large columnar ice blocks in a multi-year ridge initially formed by compression lie in a near-horizontal position. At this orientation the direction of elongation of the crystals or the columns in these large ice blocks in near vertical. The columnar ice samples collected from vertical coring will, therefore, be loaded nearly parallel to the direction of crystal elongation (σ:z=0°). This is the hard fail direction in columnar ice. Horizontally cored columnar ridge samples will tend to have an angle of 90° between the long columns and the applied load (σ:z = 90°). Work by Peyton (1966) and Timco and Frederking (1986) has shown that columnar ice samples loaded parallel to the elongated crystal axes have compressive strengths 2-4 times higher than samples loaded normal to the direction of elongation. Mixed ice samples with large fragments of columnar ice are also affected by the

orientation of the columnar ice within them. If the columnar fragments in the sample are oriented with the direction of crystal elongation parallel to the load (σ:z = 0°) the sample will fail at a relatively high load and deformation will occur in the granular material surrounding the columnar fragments. The difference between the mean compressive strength of vertically and horizontally cored samples will depend on the number of columnar test specimens in the test series and their crystallographic orientation relative to the load. The results from the tests on the matched ridge ice sample pairs are discussed in more detail in Richter-Menge and Cox (1985).

The influence of the c-axis orientation relative to the load (σ:c) on the compressive strength of the columnar samples is evident in Figure 4d. The majority of horizontal samples tested at this condition were columnar and had an angle of approximately 90° between the direction of elongation and the load, which was applied along the cylindrical axis of the test specimen (σ:z = 90°). These horizontal samples had a higher strength when σ:c was near 0°. As the σ:c angle increased the compressive strength decreased significantly. This behavior is well documented in reports on the compressive strength of horizontally cored first-year sea ice samples [Richter-Menge et al. (in prep, b), Wang (1979), and Peyton (1966)]. The first-year sea ice tests have shown that the compressive strength of horizontal samples loaded parallel to the c-axes (σ:c = 0°) is greater than the strength of samples loaded perpendicular to the c-axes (σ:c = 90°) and that both are greater in strength than a sample where σ:c = 45°.

The Phase I and II unconfined , uniaxial compressive strength data is combined in a mean strength versus strain rate plot in Figure 5. We have

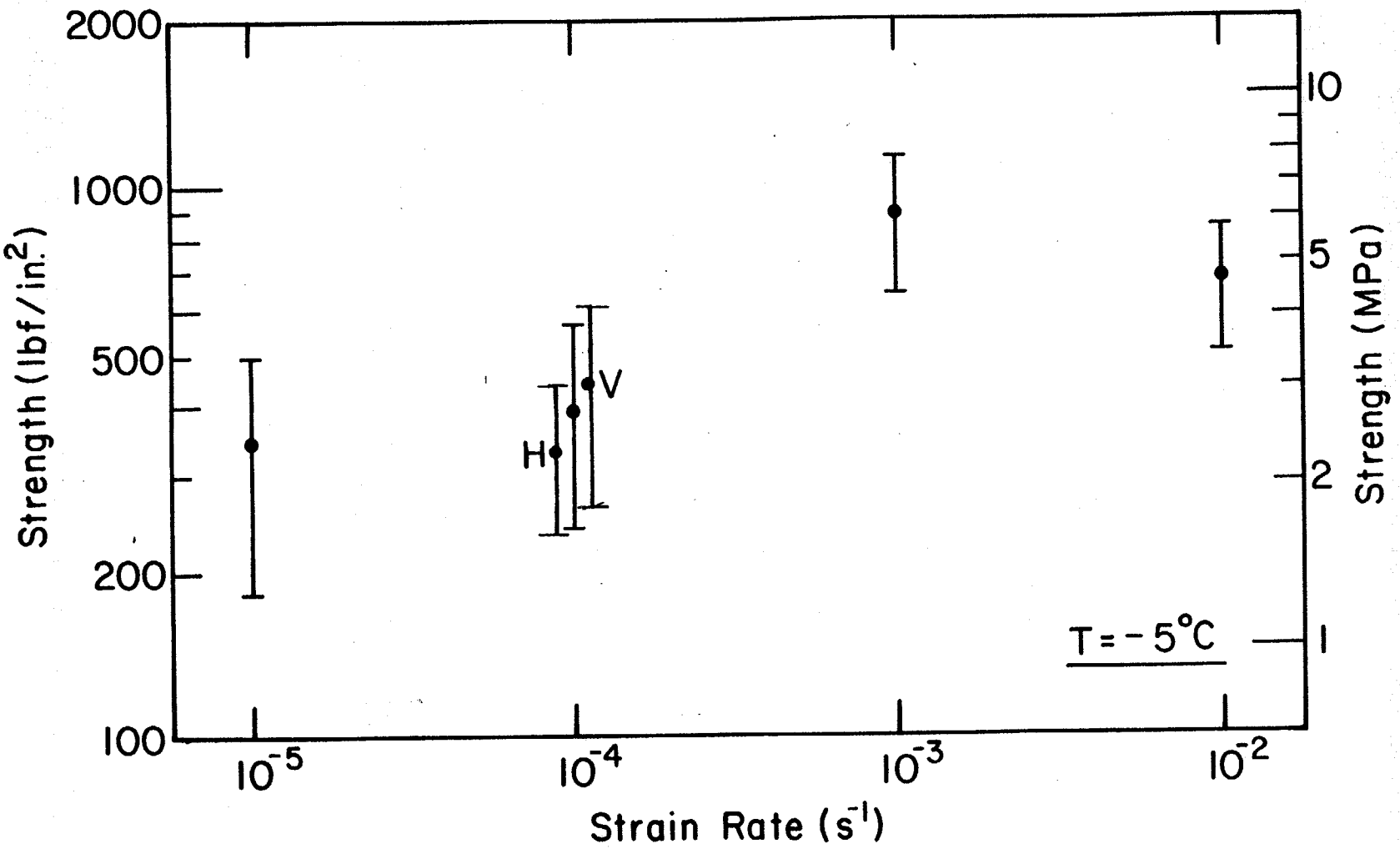

a. Samples tested at -5°C.

Figure 5. Unconfined, constant-strain-rate mean compressive strength vs strain rate. H = horizontally cored samples only, V = vertically cored samples only. The bars denote one standard deviation.

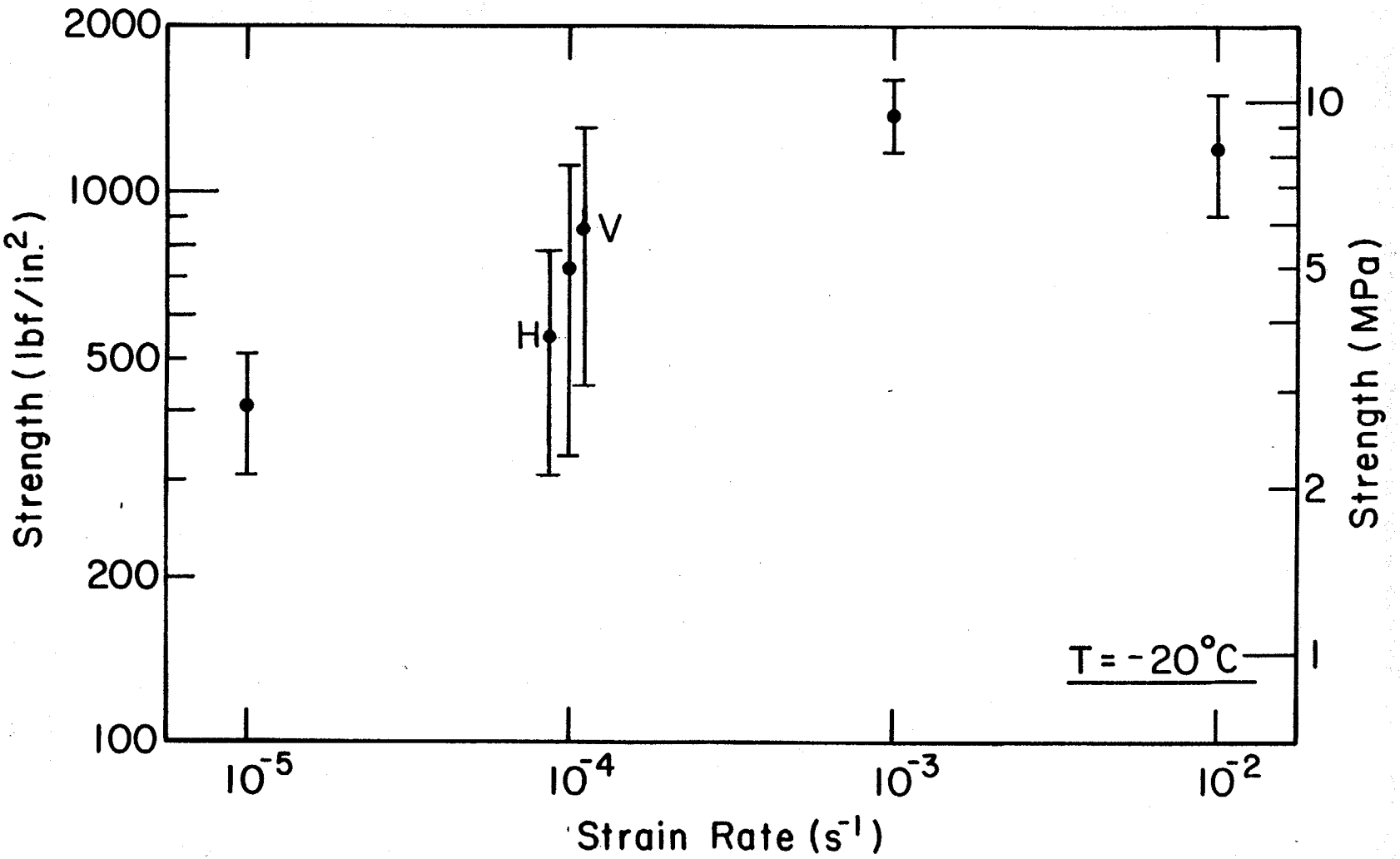

b. Samples tested at -20°C.

noted the compressive strength of the horizontal and vertical samples at 10^{-4} s^{-1} separately in the figure. All of the test specimens used at the other test conditions were from vertically cored ice. We will compare the test results from the Phase I and II vertically cored samples only since the orientation of the samples does affect the compressive strength.

As discussed in the Phase II report on test results (Cox et al., 1985), we would expect a power law relationship between ice strength and strain rate in the ductile region between 10^{-5} and 10^{-3} s^{-1} (Mellor, 1983). This relationship, which plots as a straight line on log-log paper, was not observed in our test results. The porosity variations between the Phase I and II samples appeared to explain this deviation. After analyzing the ice structure characteristics of the samples tested in each group, however, it becomes apparent that variations in the overall structural composition of each test group also affect the test results.

The Phase I structural analysis indicated that at -5°C, both the 10^{-3} and 10^{-5} s^{-1} sample groups were characterized by an isolated cluster of extremely high strength columnar samples. These columnar samples were loaded such that $\sigma{:}z \leq 10°$. The two, Phase I sample groups, tested at -20°C did not exhibit this characteristic. The structural analysis of the Phase II ice samples tested at a strain rate of 10^{-4} s^{-1} (Fig. 4b and d) shows that at -20°C there is an isolated group of extremely high strength columnar samples and at -5°C there is none. These differences are reflected in the mean strength versus strain rate plots. At -5°C (Fig. 5a), the mean strength of the 10^{-4} s^{-1} vertical samples falls below a straight line drawn between the 10^{-5} and 10^{-3} test results of Phase I. The mean strength of the 10^{-4} s^{-1} samples tested at -20°C lies above this line (Fig. 5b).

Table 4. Summary of percent granular, columnar, and mixed ice samples at each Phase II confined compression test condition.

		-5°C			-20°C		
	σ_2/σ_1	0.25	0.50	0.50	0.25	0.50	0.50
	$\dot{\varepsilon}$	10^{-5} s^{-1}	10^{-5}	10^{-3}	10^{-3}	10^{-5}	10^{-3}
Granular		30%	11	22	22	11	11
Columnar		30	11	11	11	11	0
Mixed		40	78	67	67	78	89
Total number of samples tested		10	9	9	9	9	9

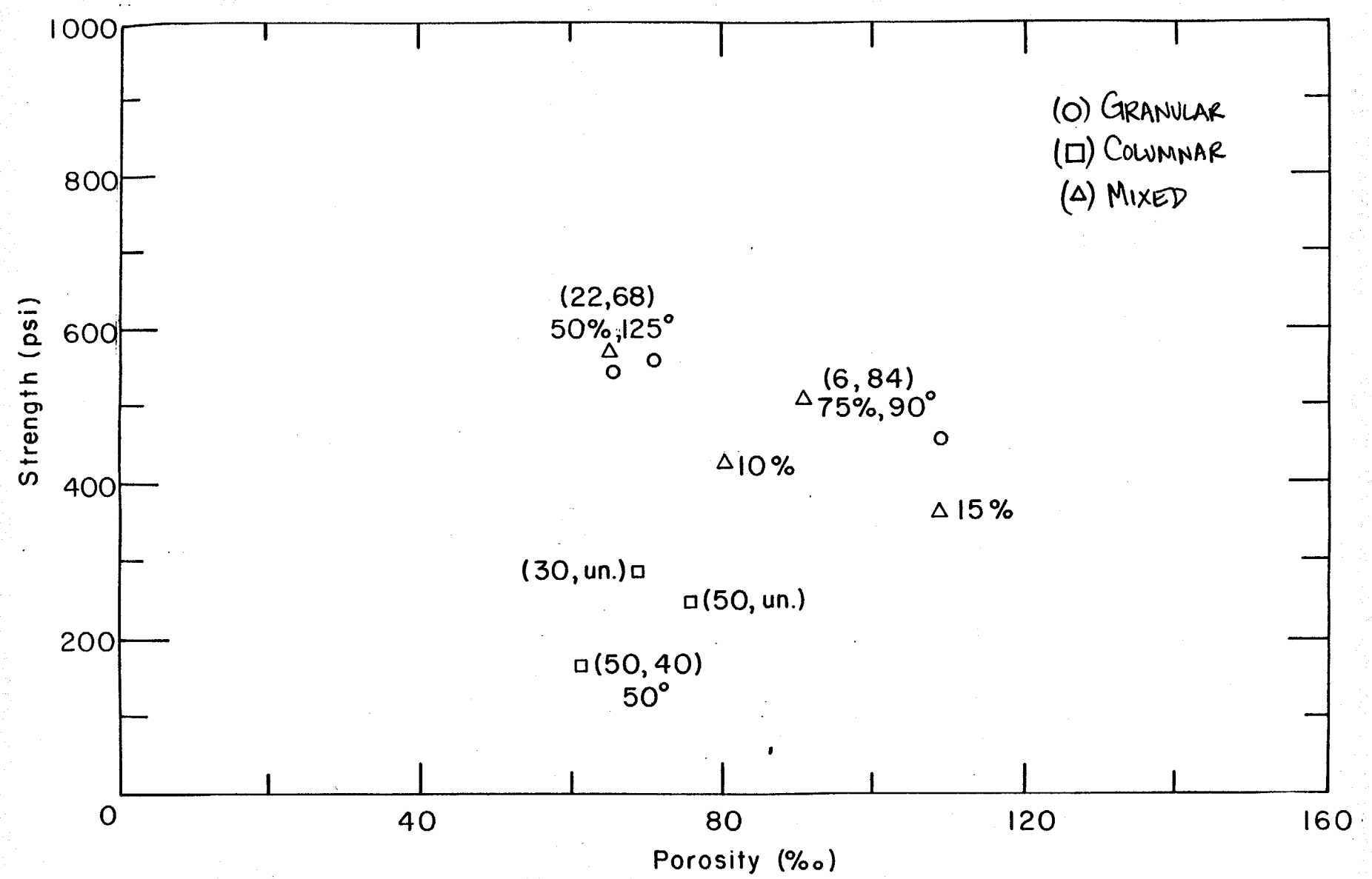

a. Phase II multi-year ridge samples tested at 10^{-5} s^{-1}, -5°C, and $\sigma_2/\sigma_1 = 0.25$.

Figure 6. Confined constant-strain-rate compressive strength vs porosity for all Phase II ridge samples with the structural classification indicated for each sample. Phase I multi-year floe test data is included when appropriate and is indicated with a closed symbol. Crystallographic measurements indicated next to each sample: (σ:z, σ:c), % columnar, °spread.

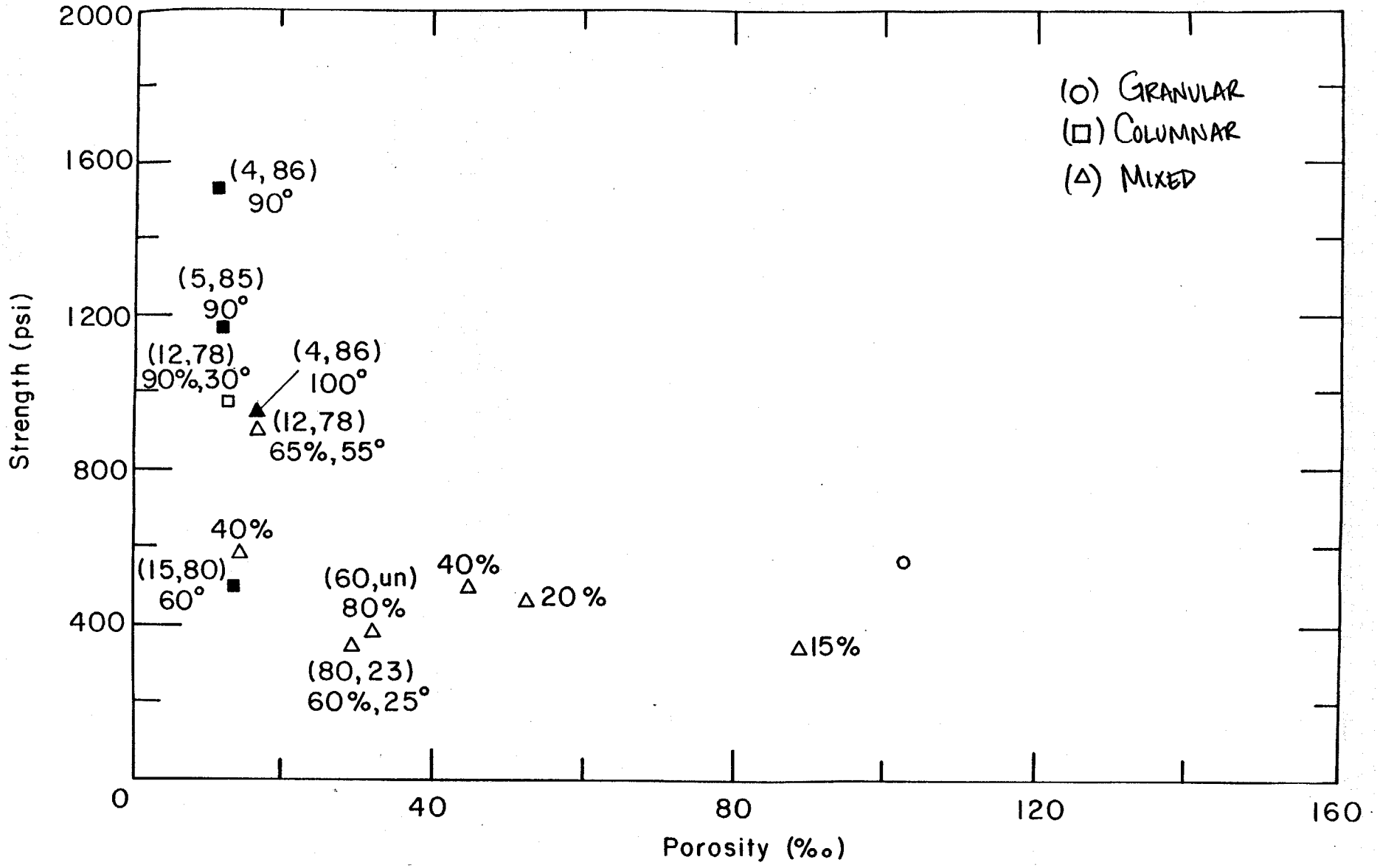

b. Phase II multi-ridge samples (open symbols) tested at 10^{-5} s^{-1}, -5°C, and $\sigma_2/\sigma_1 = 0.50$ and Phase I multi-year floe samples (closed symbols) tested at 10^{-5} s^{-1}, -5°C, $\sigma_2/\sigma_1 = 0.46$.

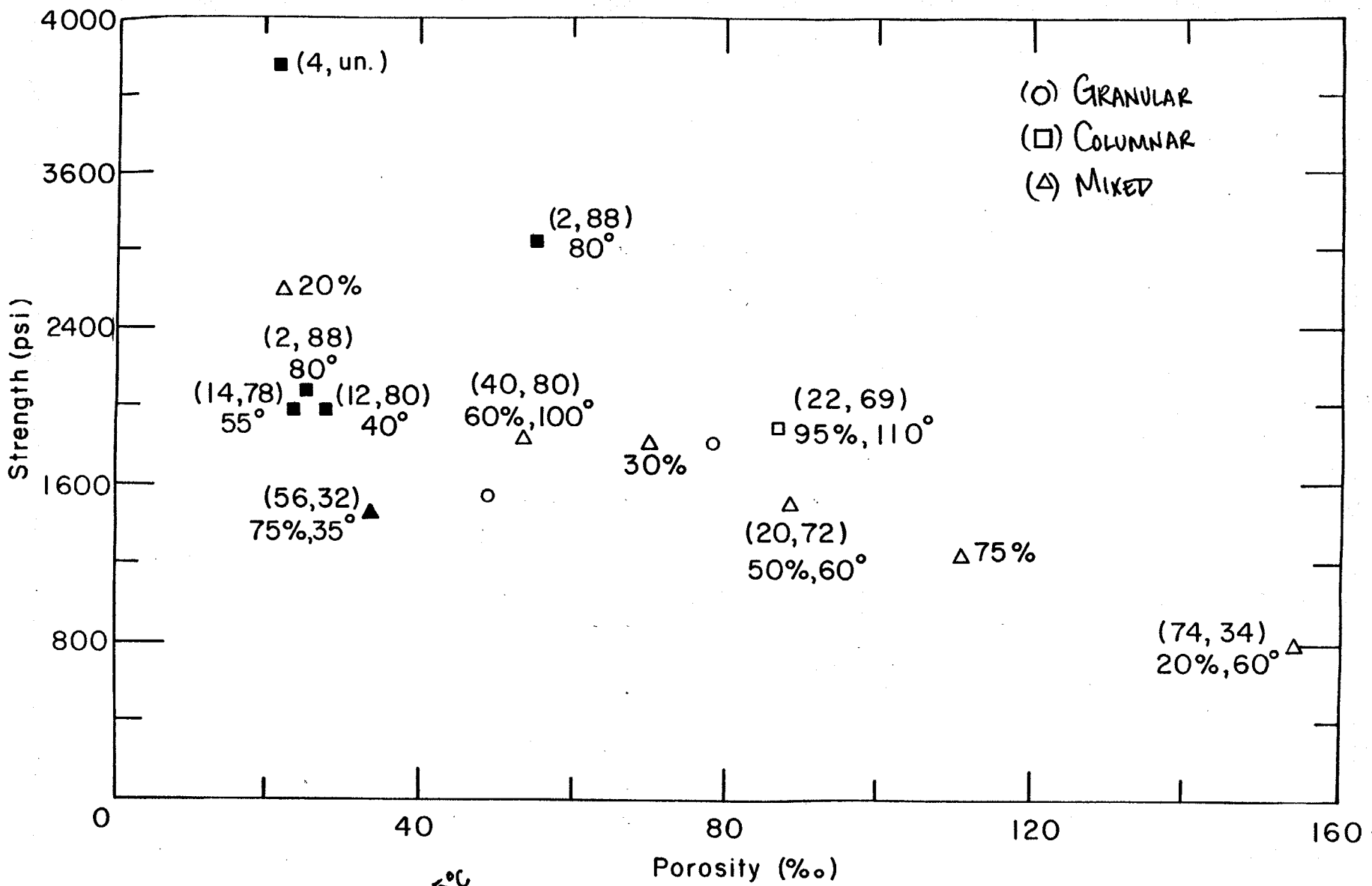

c. Phase II multi-year ridge samples (open symbols) tested at 10^{-3} s^{-1}, °C, and $\sigma_2/\sigma_1 = 0.50$ and Phase I multi-year floe samples (closed symbols) tested at 10^{-3} s^{-1}, °C, $\sigma_2/\sigma_1 = 0.46$.

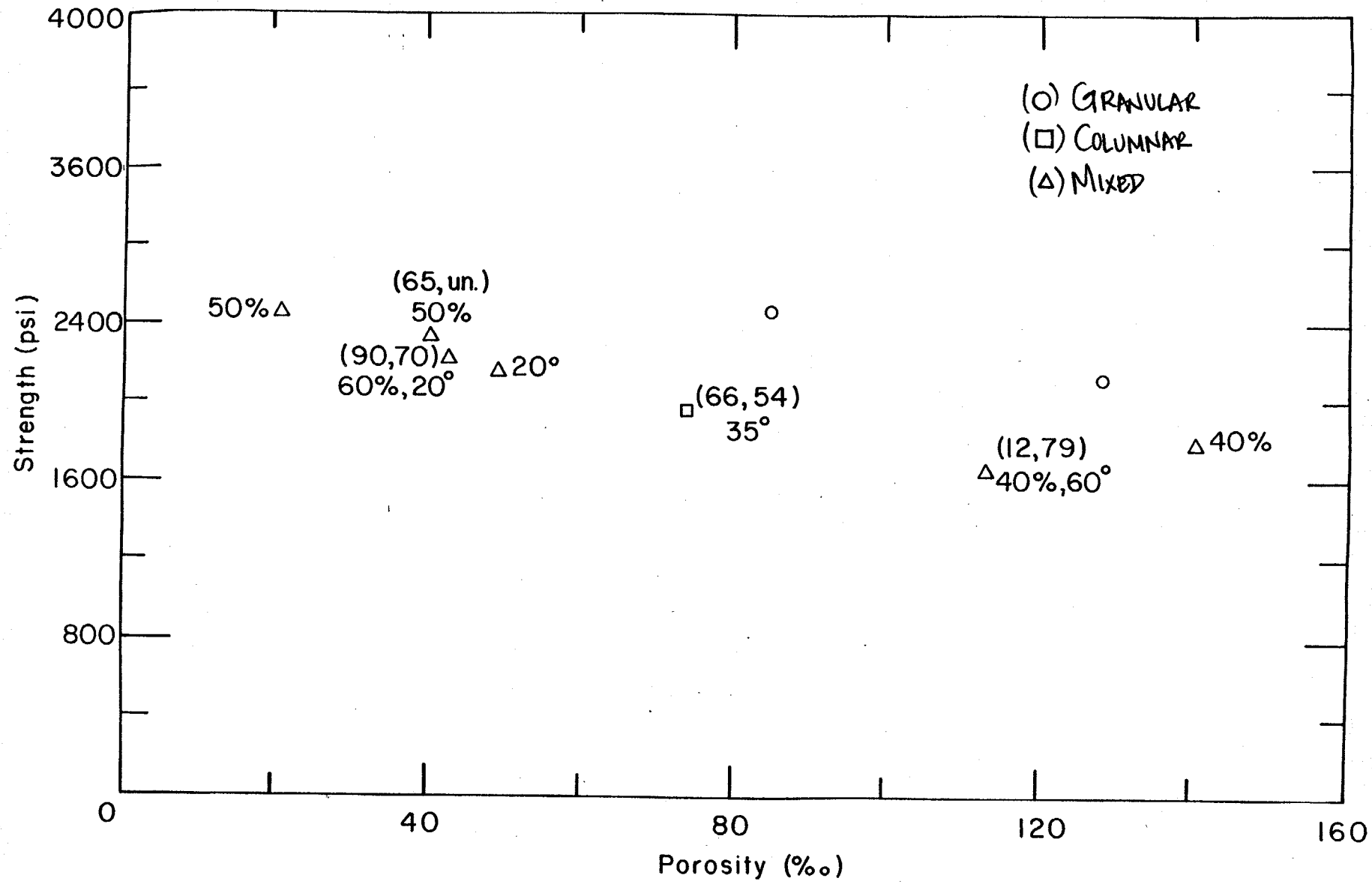

d. Phase II multi-year ridge samples tested at 10^{-3} s^{-1}, -20°C, and $\sigma_2/\sigma_1 = 0.25$.

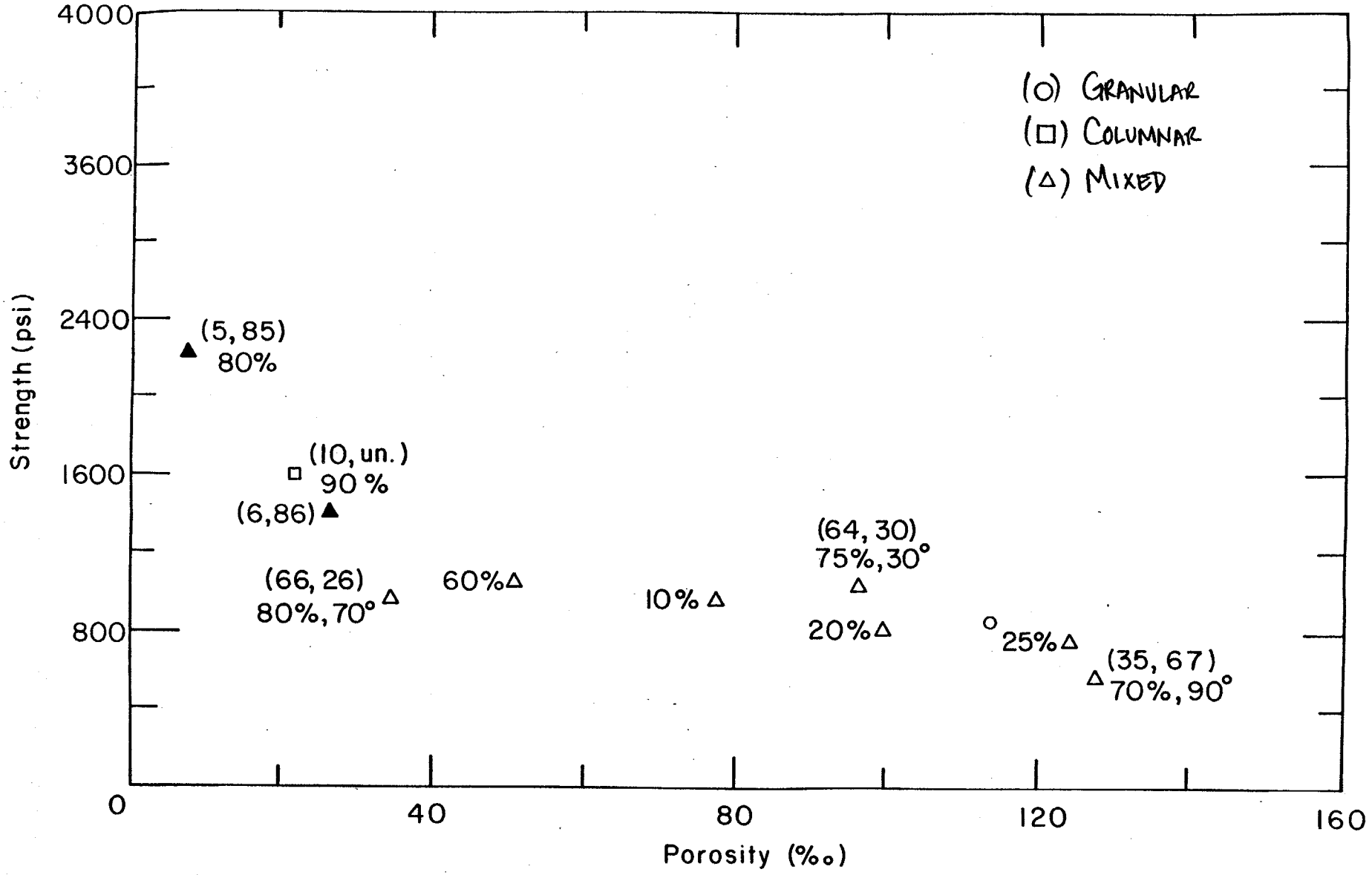

e. Phase II multi-year ridge samples (open symbols) tested at 10^{-5} s^{-1}, -20°C, and $\sigma_2/\sigma_1 = 0.50$ and Phase I multi-year floe samples (closed symbols) tested at 10^{-5} s^{-1}, -20°C and $\sigma_2/\sigma_1 = 0.46$.

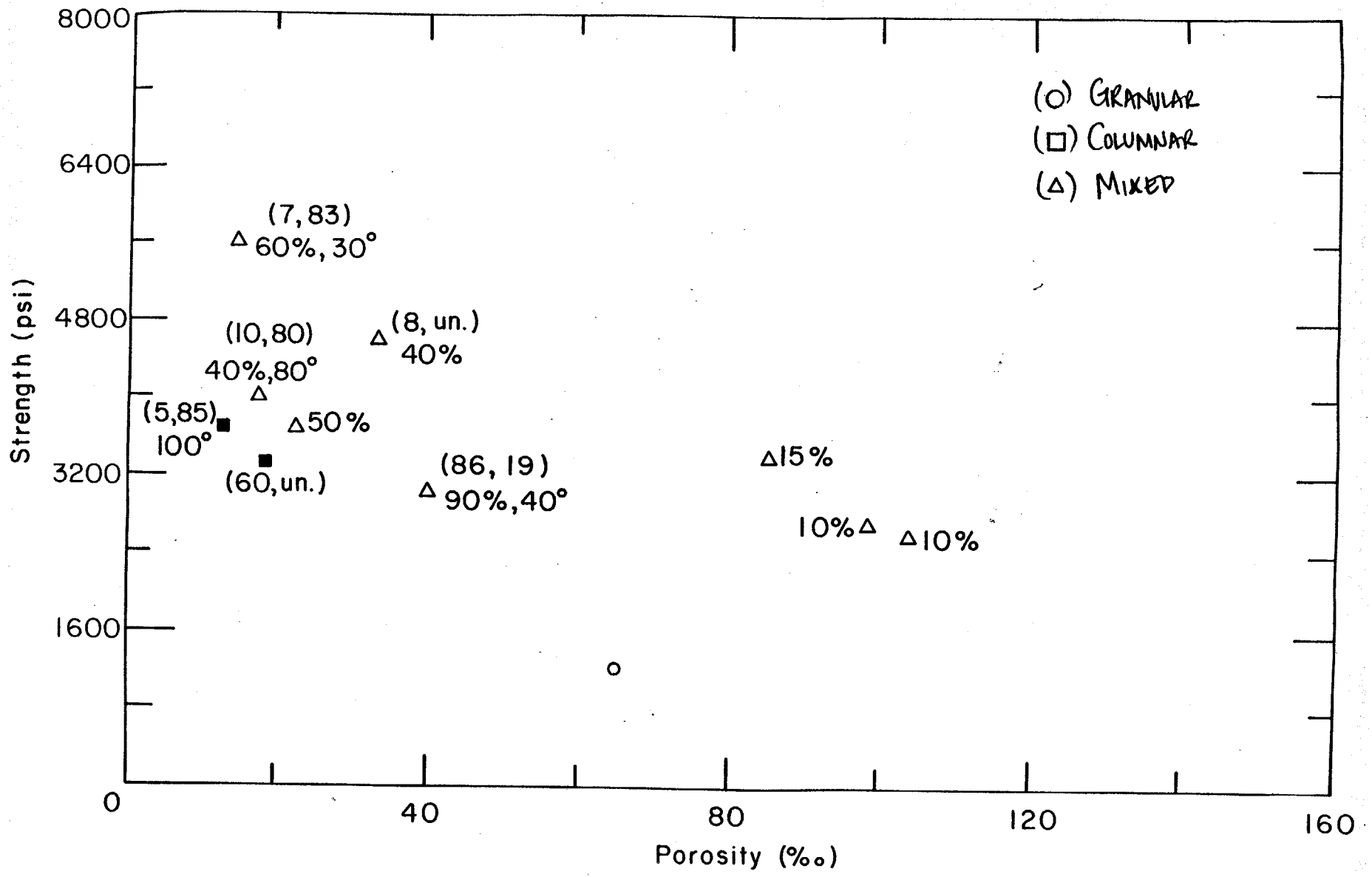

f. Phase II multi-year ridge samples (open symbols) tested at 10^{-3} s^{-1}, -20°C, and $\sigma_2/\sigma_1 = 0.50$ and Phase I multi-year floe samples (closed symbols) tested at 10^{-3} s^{-1}, -20°C and $\sigma_2/\sigma_1 = 0.46$.

The distribution of ice types at a given test condition is relatively consistent. The majority of samples consists of a mixture of columnar and granular ice, similar to the Phase I and Phase II unconfined compression test samples. There is one exception, at a strain rate of 10^{-5} s^{-1}, -5°C, and confinement ratio of 0.25, there are approximately the same number of samples in each ice type category.

We would anticipate the influence of ice structure in the confined compression tests to be similar to that observed in the unconfined compression tests given the common deformational mechanisms. In general, we did observe this to be the case. Columnar samples with a σ:z angle near 45° had a low compressive strength (Fig. 6a). There was an increase in strength as σ:z became greater than or less than 45°. The columnar and mixed ice samples from Ridge B, which were used in half of these tests, tended to have a high σ:z angle. Consequently, we did not observe any isolated groups of high strength columnar samples in the confined compression tests on the multi-year ridge samples. This should be noted when combining the results of the confined compression tests and the Phase I unconfined compression tests data to define the characteristics of the yield surface. Recall that in Phase I the columnar ice samples generally had low σ:z angles. As we discussed in the combined analysis of the unconfined compression test data from Phase I and II, differences in the overall ice structure characteristics of the test groups do affect the relative mean strengths. Addition of the multi-year floe ice samples tested in Phase I at a confinement ratio of 0.46 does show that in the confined tests, columnar samples with a σ:z angle near 0° tend to have the highest strength (Figs. 6b and c).

The confined compressive strength of mixed and granular ice samples shows a strong tendency to decrease with an increase in porosity at all test conditions. Those mixed ice samples with a high percent of columanr ice ($\geq$ 80%) lie on the outside of the strength versus porosity band. As we discussed in the previous section, this is a result of the orientation of the columnar fragments within the sample.

Uniaxial constant-strain-rate tension tests

Direct tension tests were done on 36 multi-year ridge ice samples in Phase II of the program. All of these samples failed via an extension mechanism as illustrated in Figure 2d. Tensile strength is plotted against sample porosity in Figure 7. We have included the structural classification and crystallographic measurements for the samples in this figure.

All but six of the multi-year ridge ice samples tested in tension consisted of a mixture of columnar and granular ice (Table 5). Three of the remaining samples were columnar and 3 were granular. To gain a more complete understanding of the influence of ice structure on the tensile strength of the multi-year ice, we have included the Phase I multi-year floe ice test results in Figure 7. The floe ice was predominately columnar. Based on the combined results, it appears that the tensile strength of multi-year ice shows little dependency on ice type. We do observe that the columnar ice samples tend to have a higher strength than the mixed and granular ice samples at all test conditions. We believe that this is due to the generally lower porosity of these columnar samples rather than differences in the ice type. If the columnar structure of the ice was the reason for the increased tensile strength, we would expect to see a relationship between the orientation of the columns relative to the load (σ:z)

Table 5. Summary of percent granular, columnar, and mixed ice samples of each Phase II uniazial tension test condition.

	-5°C		-20°C	
	10^{-3} s^{-1}	10^{-5}	10^{-3}	10^{-5}
Granular	0%	11	11	11
Columnar	22	0	0	11
Mixed	78	89	89	78
Total number of samples tested	9	9	9	9

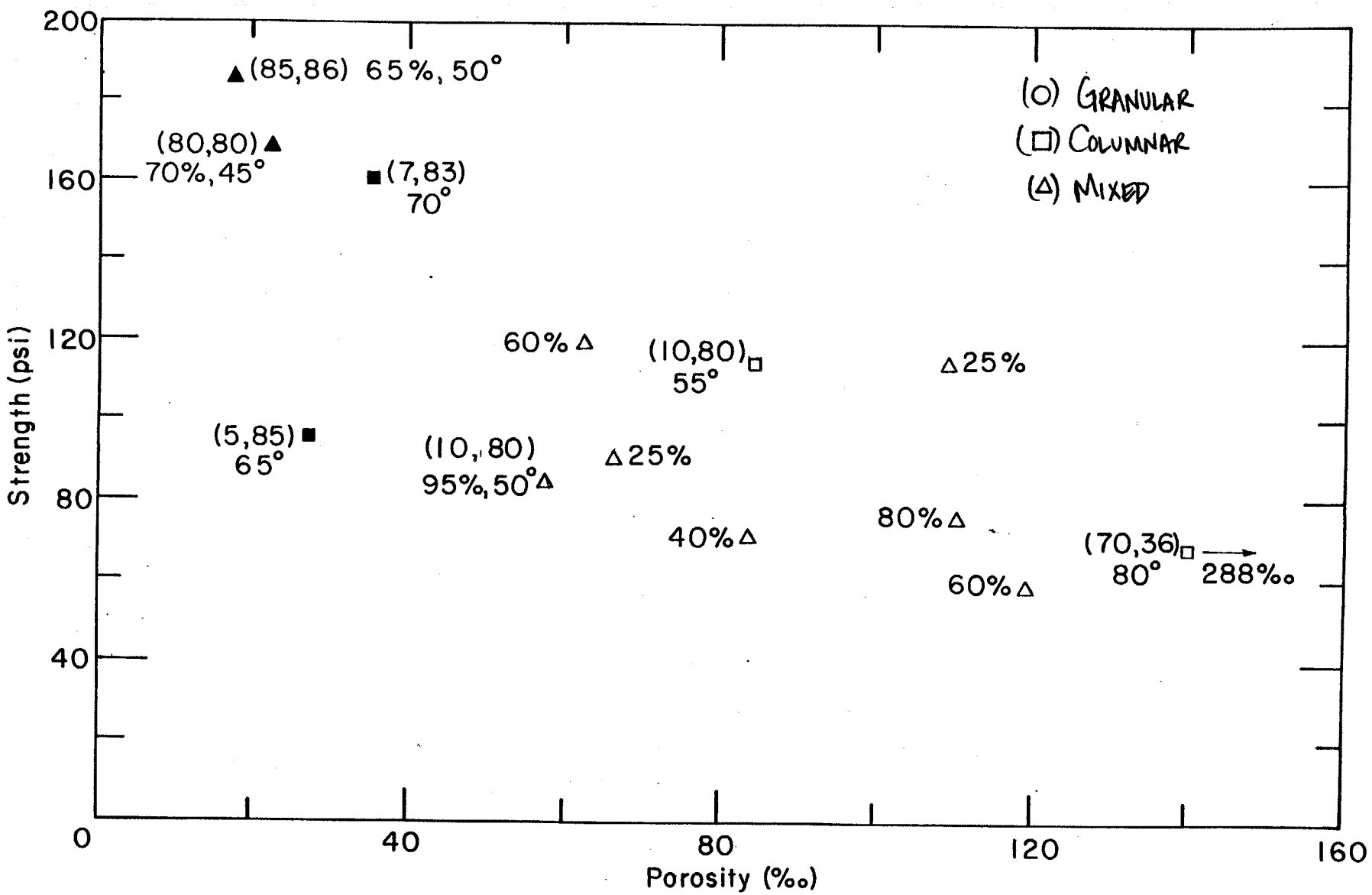

a. Samples tested at 10^{-3} s^{-1} and -5°C.

Figure 7. Constant-strain-rate tensile strength vs porosity for all Phase II ridge samples with the structural classification indicated for each sample. Phase I multi-year floe test data is included and is indicated by a closed symbol. Crystallographic measurements indicated next to each sample: (σ:z,σ:c), % columnar, °spread.

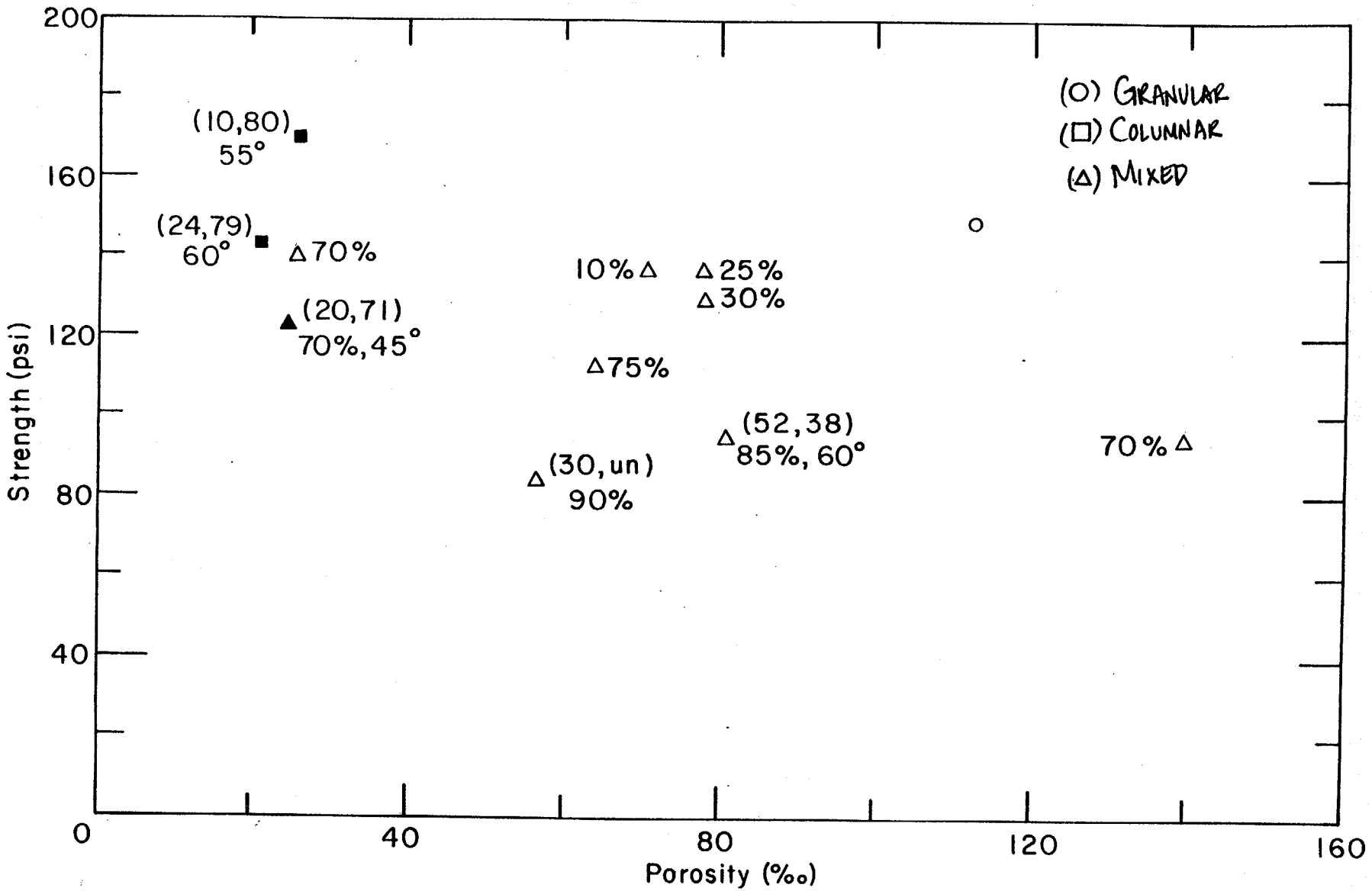

b. Samples tested at 10^{-5} s^{-1} and -5°C.

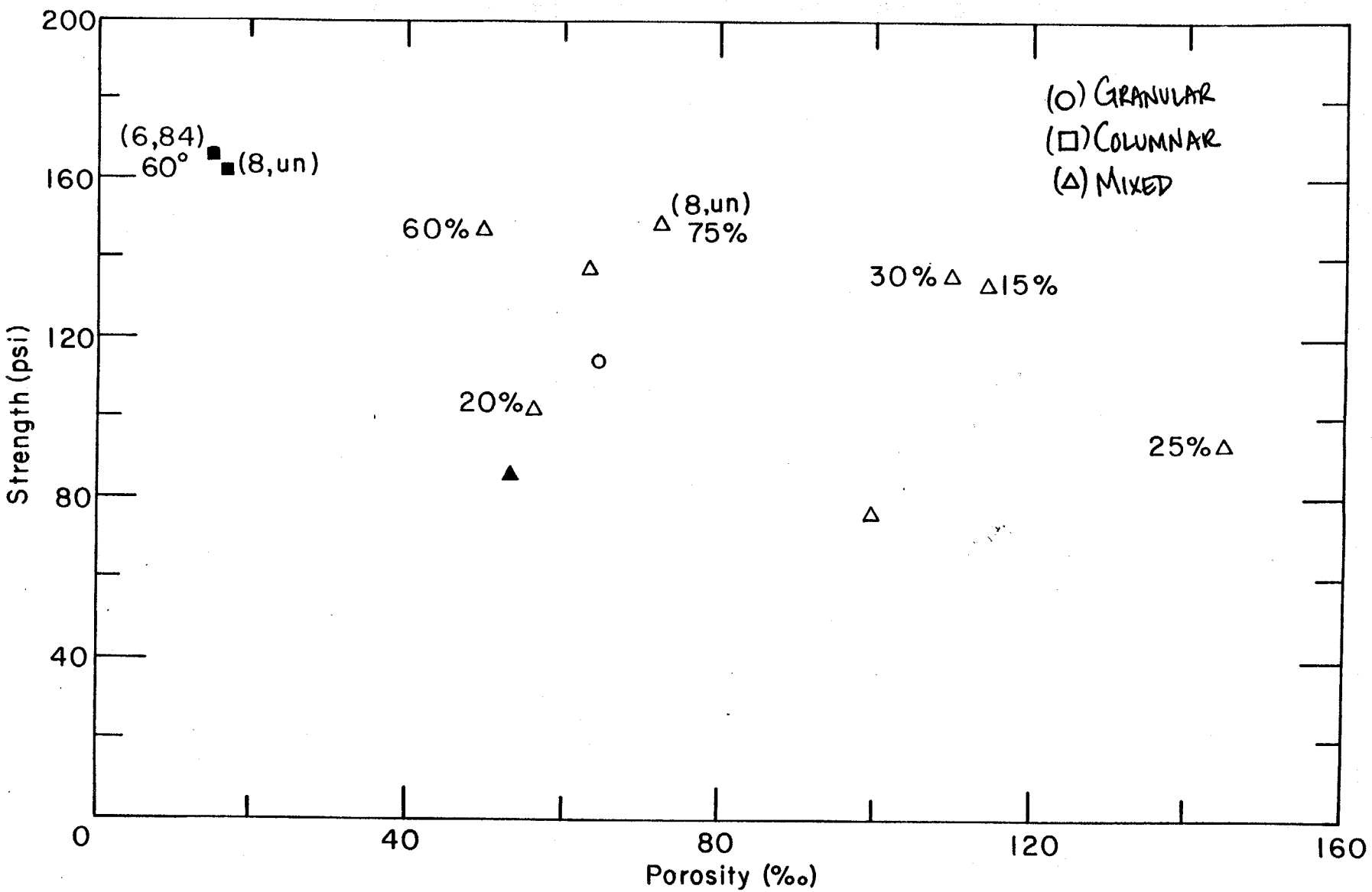

c. Samples tested at 10^{-3} s^{-1} and -20°C.

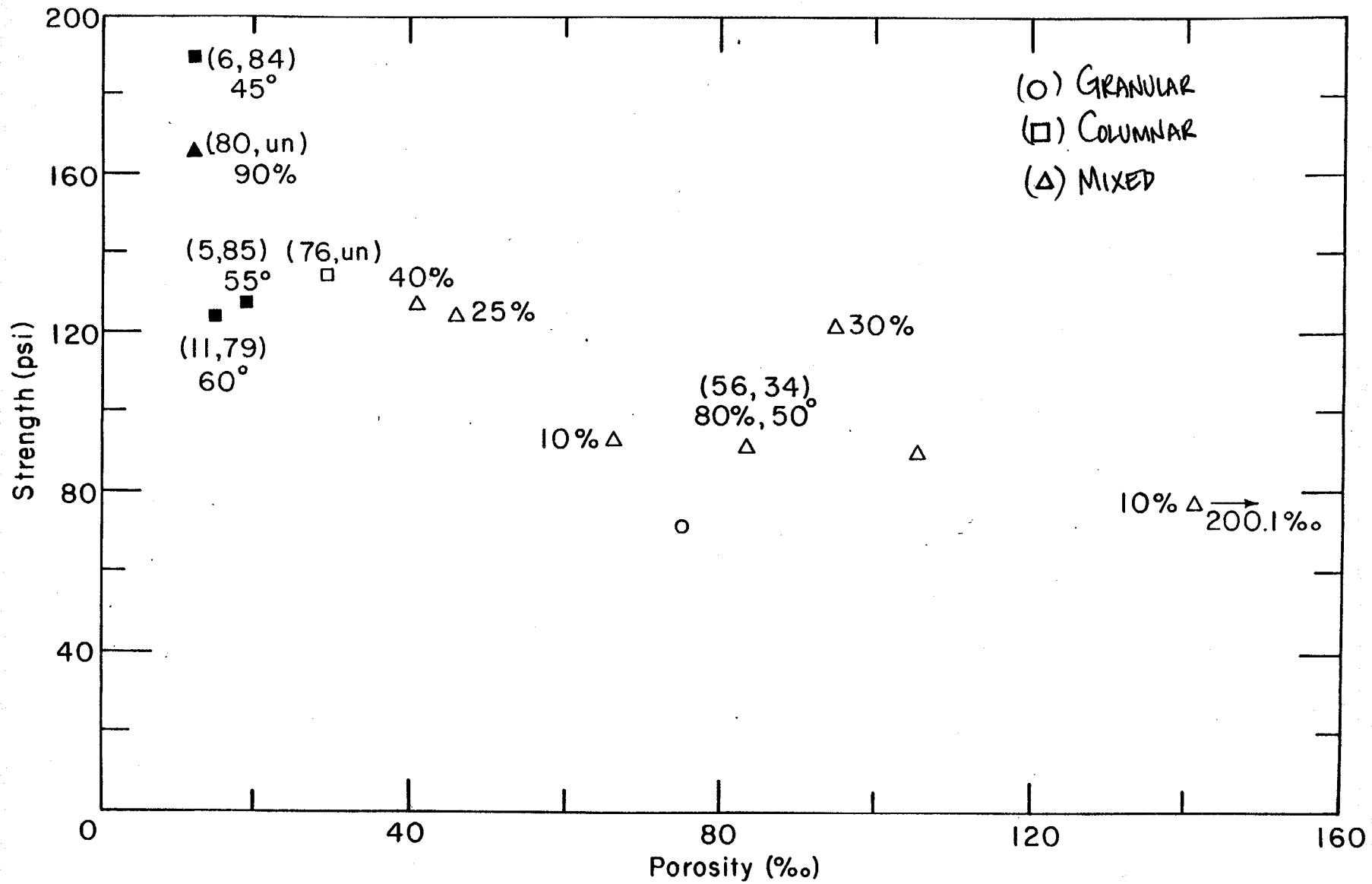

d. Samples tested at 10^{-5} s^{-1} and -20°C.

and the strength. Such a relationship has been observed by both Peyton (1966) and Dykins (1970) in tests on first-year sea ice samples. In Peyton's test the tensile strength of the ice varied from 290 psi at a σ:z orientation of 0° to 100 psi at an orientation of σ:z = 90° and σ:c = 45°. The tests by Dykins supported these findings. Our test data do not indicate this trend. We do note, however, that a columnar ice sample with a porosity comparable to a mixed or granular ice sample also has a comparable strength (Fig. 7a and d).

We also analyzed the effect of grain size on the tensile strength of the multi-year ridge ice samples. In Figure 8, we have indicated the mean grain size measured at the failure plane for each test sample. Two values next to a data point indicates that the failure plane crossed both columnar and granular ice crystals. The larger number represents the mean columnar grain size and the smaller, the mean granular grain size. Results from direct tension tests on fresh water, equiaxed polycrystalline ice (Currier and Schulson, 1982) show an inverse relationship between grain size and tensile strength. This relationship was not apparent in our test results. We did observe a tendency for the mixed samples ice to fail in the part of the specimen where the grains were coarser. There were exceptions, including mixed ice samples with columnar fragments oriented in the hard fail direction (σ:z = 0°). These samples failed in the finer-grained ice that surrounded the fragments. Other mixed ice samples failed at abrupt changes in ice structure. One consistent observation was the coincidence of failure planes with large ($\geq$ 1 cm), isolated voids in the samples. The samples that failed at structural discontinuities and voids are indicated in Figure 8.

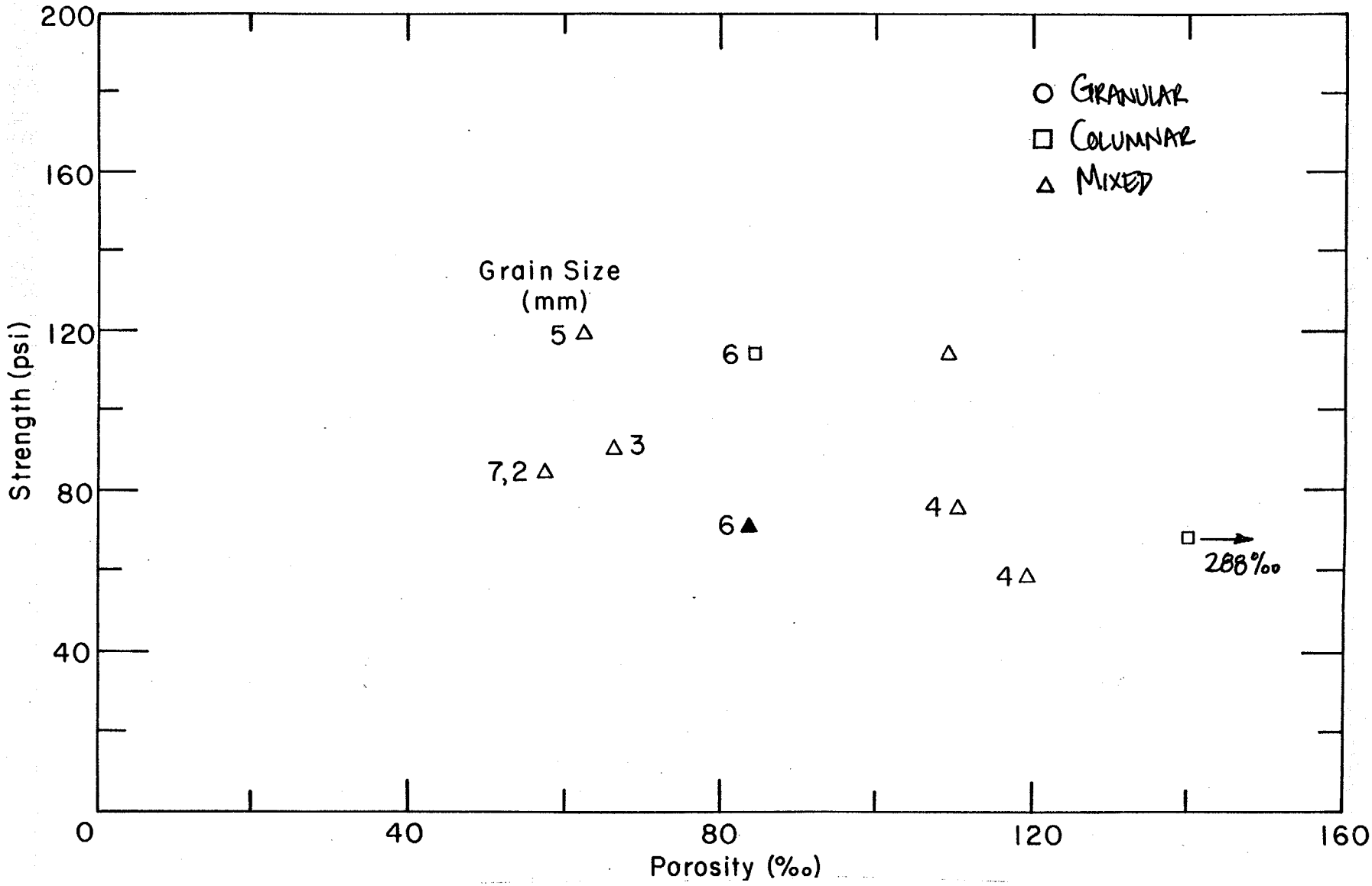

a. Samples tested at 10^{-3} s^{-1} and -5°C.

Figure 8. Constant-strain-rate tensile strength vs porosity for all Phase II ridge samples with the structural classification indicated for each sample. The mean grain size (mm) at the failure plane is given next to each sample. Failure at an abrupt change in ice type is denoted by a

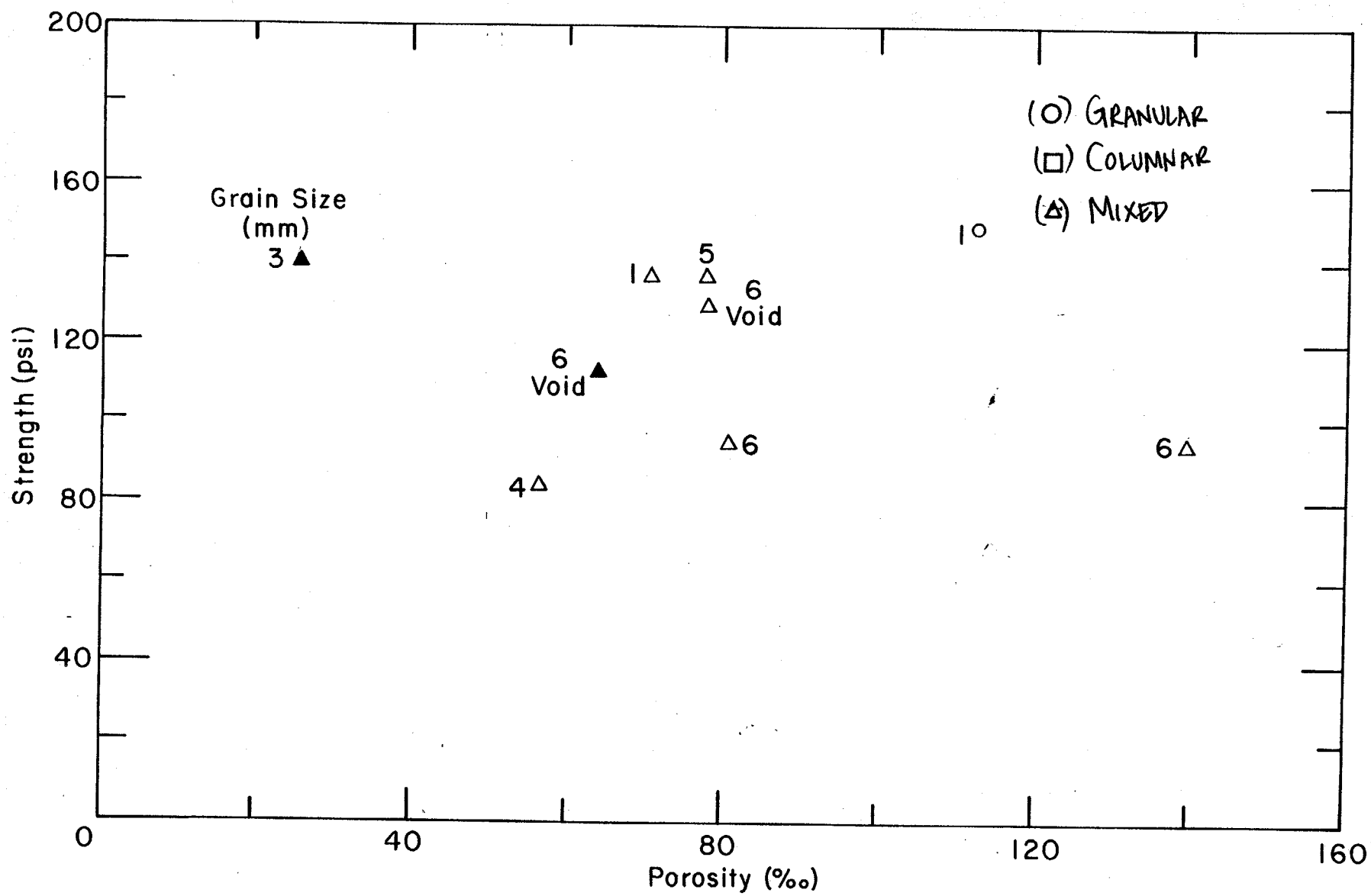

b. Samples tested at 10^{-5} s^{-1} and -5°C.

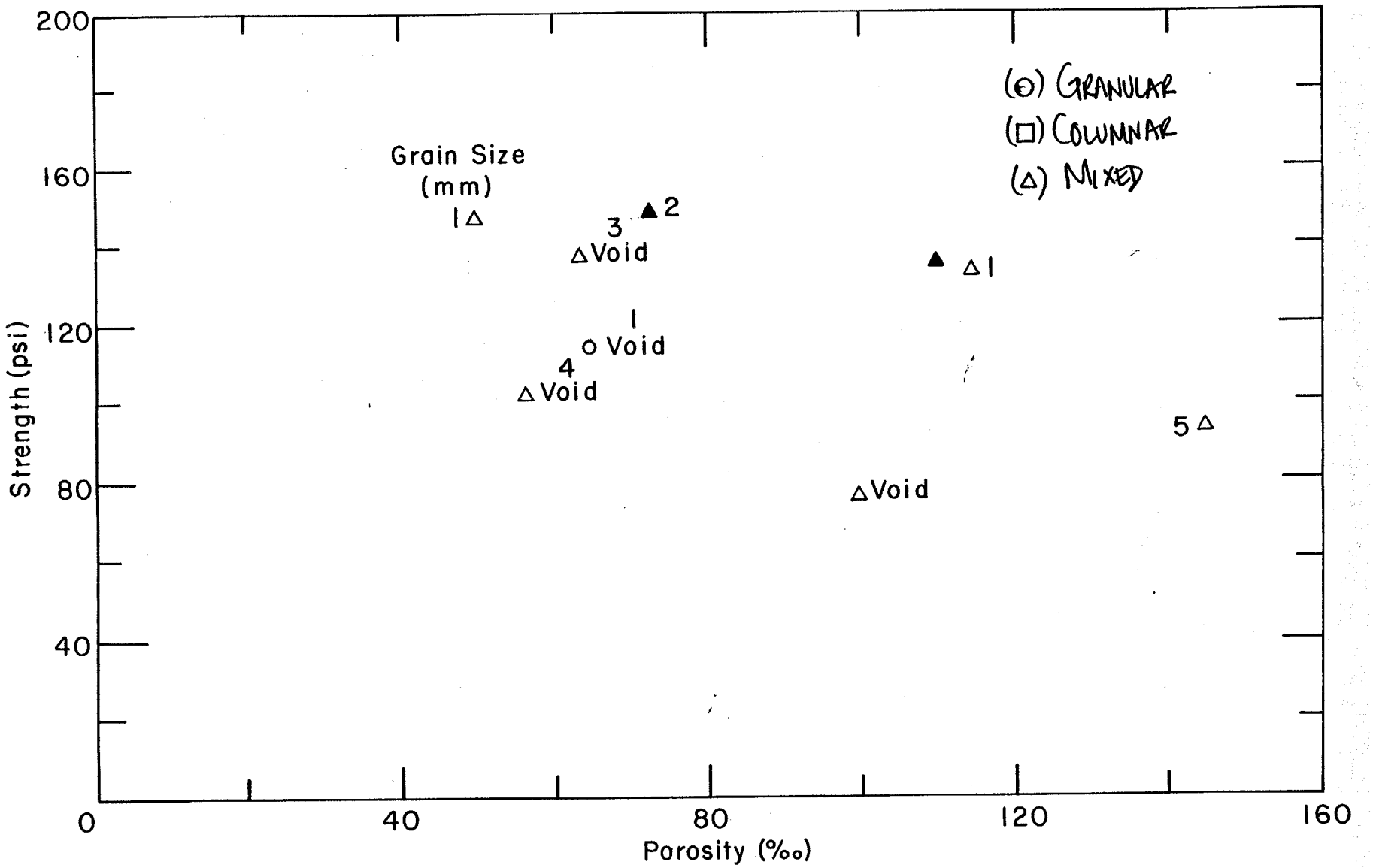

c. Samples tested at 10^{-3} s^{-1} and -20°C.

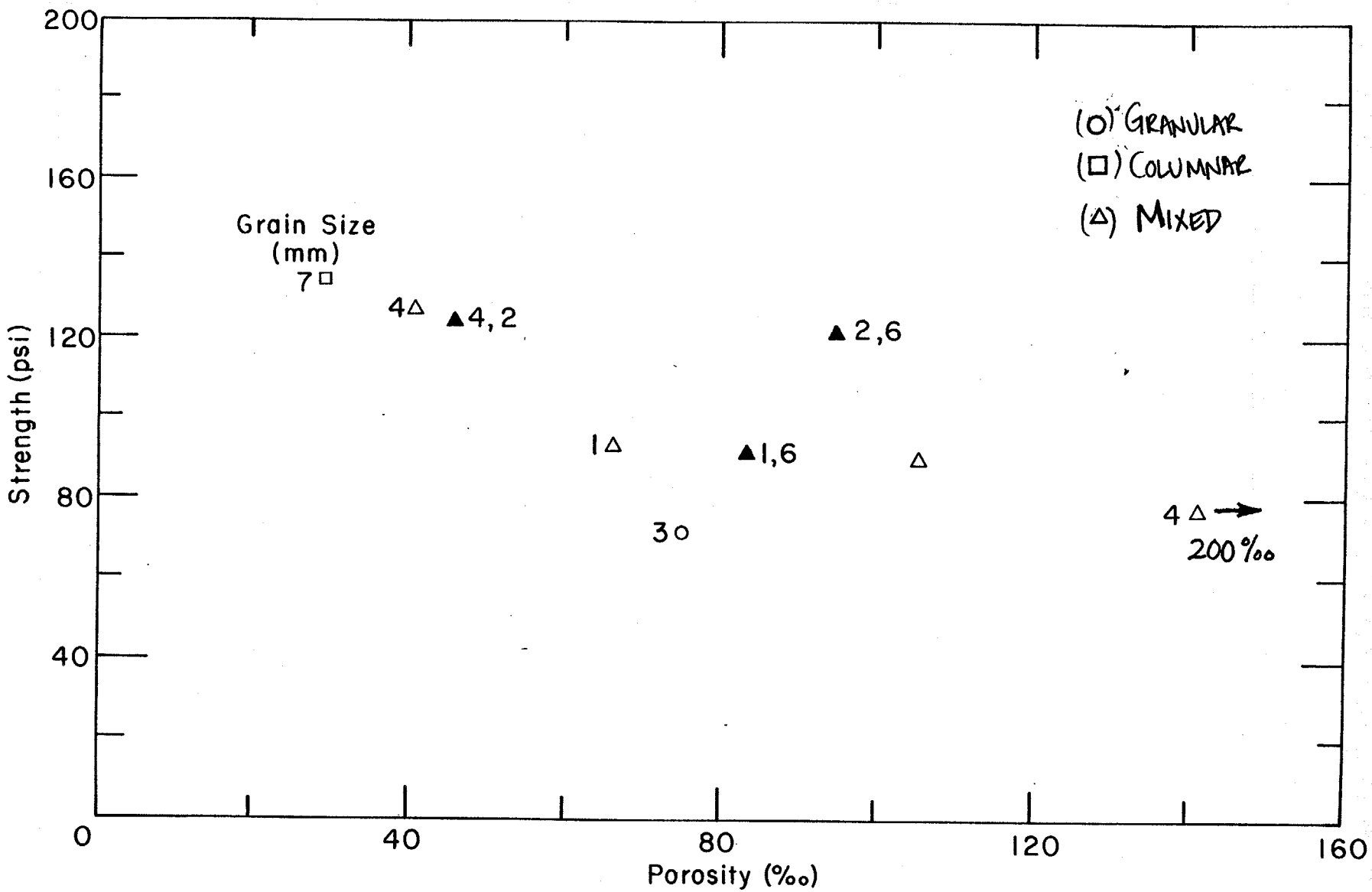

d. Samples tested at 10^{-5} s^{-1} and -20°C.

It becomes apparent on these plots that while the location of the failure plan may be influenced by grain size, changes in the ice structure, and large voids, the tensile strength of the samples is not. Instead, the porosity of the sample seems to be the dominant characteristic influencing the tensile strength of the multi-year ridge ice samples. This is true at all test conditions.

DISCUSSION

A total of 14 multi-year pressure ridges have been sampled in the course of this mechanical properties test program. We have structurally analyzed ice test specimens from 13 of these ridges. In Table 6, we list the number and percent of columnar samples tested in each of the ridges. We have included as columnar those samples classified as mixed that are made up of $\geq$ 80% columnar ice. Our Phase I and II test results suggest that these mixed ice samples behave similarly to the columnar ice samples.

The amount of columnar ice varies from ridge to ridge. As we discussed in the Phase I ice structure analysis report, we believe this is due to differences in the mode of formation of the ridge. Ridges initially formed by the compression of one first-year ice sheet against another contain large blocks of columnar ice. The ice in a ridge formed by shearing on the other hand, is highly fragmented. Samples taken from ridges should reflect these differences. We would expect to get a higher percentage of columnar samples from a multi-year pressure ridge formed by compression than from one formed in shear.

A frequency histogram of the number of columnar samples in a given σ:z orientation is presented in Figure 9. The frequency histogram of the Phase I columnar samples was originally presented and discussed in Richter-Menge

Table 6. Columnar ice samples tested in Phase I and II. These samples include both columnar and mixed samples with $\leq$ 80% columnar ice.

Ridge no.	Total number of samples tested	Total number of columnar samples	% Columnar samples
	Phase I		
1	23	13	57
2	24	4	17
3	22	3	14
4	22	6	27
5	22	5	23
6	12	0	0
7	23	6	26
8	24	15	63
9	24	1	4
10	24	8	33
	Phase II		
A	46	1	2
B	54	9	17
C	53	20	38
	373	91	24

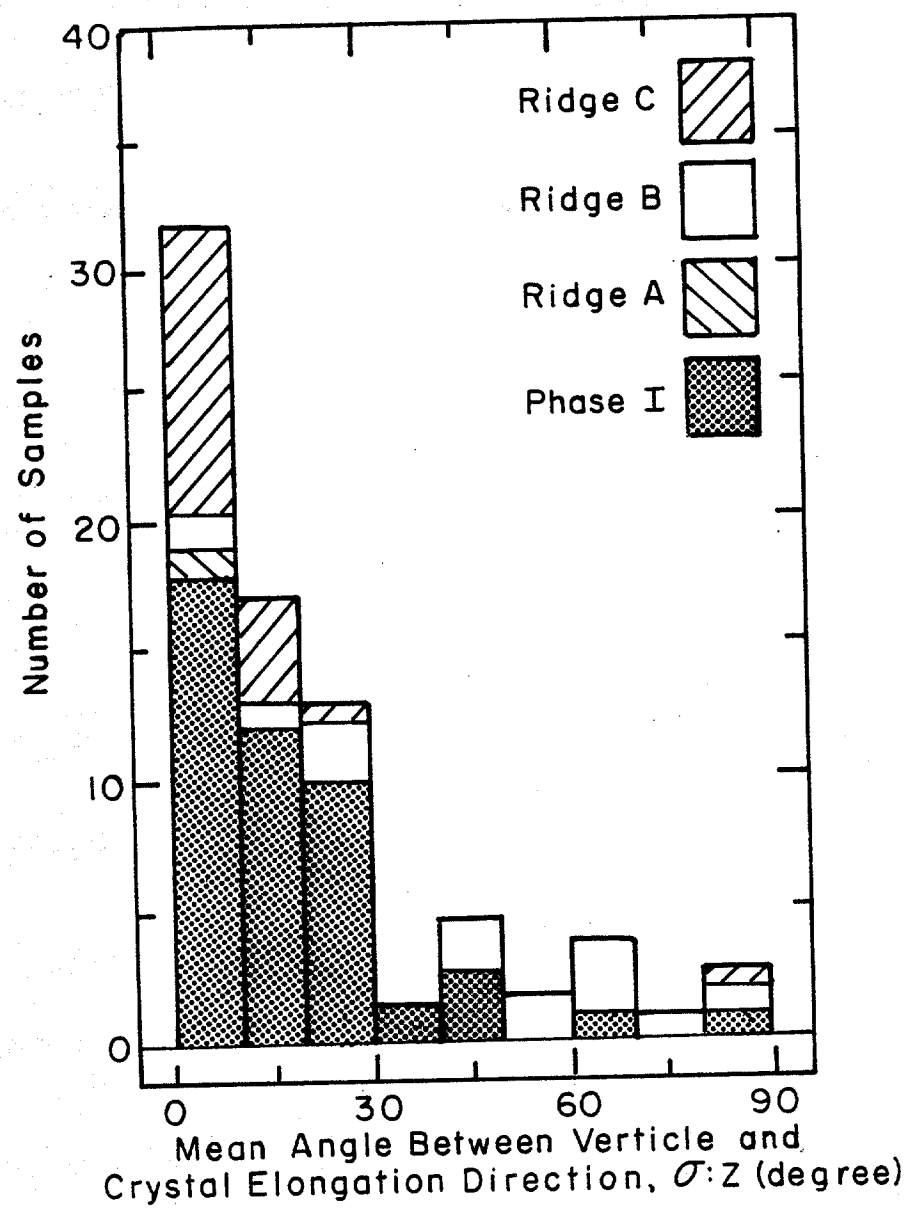

Figure 9. Frequency histogram of the Phase I and II columnar ridge ice samples in a given σ:z orientation.

et al. (in prep, a). In that report we noted the relatively large number of low σ:z measurements. Based on this observation, we concluded that in the 10 ridges we sampled during Phase I the blocks of columnar, first-year sea ice that were incorporated into the ridge during its formation, were lying in a near horizontal position. The vertically cored, columnar samples taken from these ridges tended to have a high compressive strength since they were loaded in the hard fail direction (σ:z = 0°). We further anticipated that the mean compressive strength obtained from a series of tests on vertical ridge samples would be higher than the mean value obtained from horizontal samples. The horizontal columnar samples would tend to be loaded normal to the elongated crystal axis (σ:z = 90°), giving a lower compressive strength and, hence, a lower overall mean strength. The difference would be strongly dependent on the amount of columnar ice in the test series and the orientation of the columnar ice crystals.

The Phase II unconfined compression tests on matched horizontal and vertical pairs collected during the second field program confirmed our hypothesis (Richter-Menge and Cox, 1985). As we discussed earlier in this report, we found the effect of sample orientation on the mean compressive strength of multi-year ridge ice samples tested at a given condition to be significant (Fig. 4b and d). The difference was greater in the test series with a higher percent of columnar samples (Fig. 4d).

The results of the compression tests on matched horizontal and vertical pairs would probably have been different, however, had we taken our samples from Ridge B. The samples taken from this ridge tended to have a high σ:z angle as indicated in Figure 9. Our compression test results on the ridge samples suggest that columnar samples with a σ:z angle near 45°

are generally weaker than mixed or granular ice samples with comparable porosities. Columnar samples with $15° < \sigma{:}z < 35°$ or $55° \leq \sigma{:}z < 90°$ have strengths comparable to the mixed ice samples. We would therefore, expect the mean compressive strength of vertically cored samples taken from Ridge B to be comparable to the strength obtained from horizontal samples.

Based on our sampled ridge population, it still appears that the columnar blocks within a ridge tend to be in a near horizontal direction with the elongated crystal axis near vertical. The characteristics of the Ridge B columnar ice samples show us, however, that this is not always the case. This obervation again points out the importance of the ice structure analysis for the interpretation of multi-year ice data. Each data group is unique with respect to the number of granular, columnar, and mixed ice samples and the orientation of the columnar ice within the samples. These variations in ice structure combined with differences in porosity will be reflected in the mean strengths. Without a thorough structural analysis of the ice types in all of the test groups, the combined results of a program could lead to erroneous conclusions. This is particularly true with respect to the compressive strength of the ice, both unconfined and confined. Our results on the strength of the multi-year ridge ice samples loaded in tension suggest that for strain rates from 10^{-5} to 10^{-3} s^{-1} and temperatures between -20 and -5°C, the tensile strength is insensitive to ice type. More tension tests should be done on ridge samples to confirm this observation as we tested only nine samples at each test condition. This is an extremely small number of tests given the variability of the material.

Ideally, we should be able to devise a system that allows us to adjust each data set to reflect the number of granular, columnar, and mixed ice samples that would be found in a 'representative' population of multi-year ridge samples. Orientation of the columnar ice samples would also have to

be normalized. We would then be more certain of our conclusions made on the basis of combined data sets. It appears that this could be done by weighting the results of each test. The difficulty comes in defining the representative sample population. We expect it to be a function based on the number of ridges sampled and the number of samples taken from each ridge. Our current data set, involving data from 13 ridges, obviously is still too small to define this function with any certainty.

CONCLUSION

The ridge building process itself appears to be extremely dynamic based on the large percentage (approximately 80%) of mixed ice samples in our combined Phase I and II data set. It also appears that there may be a preference for the columnar ice blocks in a ridge to lie in a near horizontal position. This results in a dependency between mean compressive strength and sample orientation. Vertically cored samples tend to give a higher mean compressive strength than horizontal samples.

At the end of the first phase of this testing program it had become apparent that the ice structure in multi-year ridge samples was extremely variable and that the structure had a profound effect on the mechanical properties of the ice. The Phase II test results confirm this observation.

The ice structure analysis of the Phase II unconfined and confined compression tests shows that the effect of ice structure on the compressive strength of multi-year ridge ice samples is independent of the temperature, strain rates, and confining ratios that we used in our test series. We will, therefore, restate the following general conclusions made in the Phase I report:

- For columnar ice samples, the dominant characteristic that influences sample strength is crystal orientation. Columnar samples with the direction of crystal elongation near vertical and with a high degree of crystal c-axis alignment will have extremely high compressive strengths. When the direction of crystal elongation coincides with the direction of maximum shear at an angle of 45° to the load, the columnar samples have a very low compressive strength.
- A sample composed of both columnar and granular ice (classified as a mixed ice sample) will exhibit mechanical properties that are similar to a columnar sample if it contains 80% or more columnar ice.
- The orientation of the columnar fragments in a mixed ice sample influences the overall compressive strength and deformational characteristics of the sample. If the columnar fragments are oriented in a hard fail direction the sample will have a relatively high strength. Failure in these samples will occur in the granular material surrounding the columnar fragments.
- Mixed and granular ice samples show a significant decrease in strength with an increase in ice porosity.

The tensile strength of the multi-year ridge ice samples does not appear to be significantly influenced by ice structure. Rather, the porosity of the sample is the dominant characteristic with respect to strength.

The most significant conclusion drawn from this study is the importance of characterizing the ice structure of each test specimen. Without such an analysis, the development of a constitutive law for multi-year

ridge ice based on the data from mechanical property tests on ridge samples will be misleading. An ice structure analysis should become a standard procedure in all multi-year ridge programs. We also suggest the compilation of ice structure data taken in field sample and testing programs from all available sources. This would provide an opportunity to determine representative ridge characteristics and, hence, the overall strength that should be used in design codes.

APPENDIX A. Multi-Year Ridge Sample Data

This appendix contains the results from the ice structure analysis of the Phase II tests performed on multi-year ridge ice samples. These tests included unconfined and confined constant-strain-rate compression tests and uniaxial constant-strain-rate tension tests. The test type is denoted by UC, CC, and UT, respectively. STR. CC. -3-5/0.5 indicates the structural analysis of the confined compression tests done at a strain rate of 10^{-3} s^{-1}, a temperature of -5°C, and a σ_2/σ_1 confinement ratio of 0.5. A similar strategy was used to identify all other test condition. The parameters listed for each test are identified in Index A. The sample number RA01-262/289 gives the location and depth of the sample; that is, Ridge A, hole 1, at a depth of 262 to 289 cm. At a strain rate of 10^{-4} s^{-1} and temperatures of -5 and -20°C in the unconfined compression tests, we tested matched pairs of vertically and horizontally cored ice samples. The vertical samples are labeled with a V and the horizontal samples with an H. All of the other sampels in the Phase II portion of the test program were vertically cored.

INDEX A

Column Number

Comp.	Tension	Sympol	Description
1	1	σ_m(psi)	Peak stress or strength.
1	1	ε_m(GL)(%)	Strain at σ_m determined by DCDTs over a gauge length of 5.5 in. for the unconfined compression tests, 10.0 in. for the confined compression, and 4.5 in. for the tension tests.
3	3	t_m(s)	Time to peak stress.
4	4	E_i(GL)(10^6 psi)	Initial tangent modulus determined using strains found over the gauge length.
5	-	t_e(s)	Time to end of test.
6	-	σ_e/σ_m	Ratio of end stress at 5% full sample strain to peak stress.
7	5	n ($o/_{oo}$)	Sample porosity at test temperature.
8	6	Classification	Classification of ice texture type as granular (1), columnar (2), or a mixture of granular and columnar (3).
9	7	% Columnar	Estimation of % columnar ice in the sample.
10 11 12	8 9 10	min (mm) max (mm) mean (mm)	Measurement of the minimum, maximum, and mean columnar grain size as measured across the width of the grain.
13	11	σ:z (degree)	Angle between the direction of crystal elongation and the load applied along the cylindrical axis of the sample.
14	12	σ:c	Angle between the load and the mean crystal c-axis direction.
15	13	° spread	Degree of alignment of the c-axis. UN and R represent unaligned and random, respectivly.

16 17 18	14	min (mm) max (mm) mean (mm)	Measurement of the minimum, maximum, and mean granular grain size.
19	--	Type failure	Dominant failure mode. L = longitudinal splitting, S = shear, and MS = multiple shear failure.
20	17	Location	Location of failed area in sample. T = top, M = middle, and B = bottom of sample.

FILE 'STR.UC.-2-5

SAMPLE #.	01	02	03	04	05	06	07	08	09	10	11	12	13	14	15	16	17	18	19	20
RA01-262/289	820	.10	.14	.709	.14		64.1	3B	25	2	10	6				4	.5	1.5	S	T-M
RA06-131/158	390	.05	.07	.785	.07		150.6	3	45										S	M
RA06-337/364	621	.07	.11	.869	.11		110.9	3											S	M
RC29-112/139	708	.07	.09	.992	.09		29.5	2A	100										S	T
RC29-179/206	716	.08	.11	.974	.11		43.9	3A											S	B
RC29-342/369	470	.02	.08	.840	.08		67.1	3					B-70 30	30 70	27 (80%)-B 20 (20%)				S	M
RC31-125/152	788	.08	.13	1.000	.13		50.7	3											S	M
RC31-197/224	645	.07	.12	.975	.12		68.8	3											S	T-M
RC31-278/305	931	.08	.12	.995	.12		27.5	2A											S	M

FILE STR.UC.-4-5

SAMPLE #	01	02	03	04	05	06	07	08	09	10	11	12	13	14	15	16	17	18	19	20
RC32-133/160V	330	.15	16.50	.771	500	.591	78.8	3B	50									.5	MS	M
RC43-150H	386	.11	10.60	.739	500	.578	104.0	3B	20									.5	MS	M
RC33-205/232V	478	.10	7.80	.983	500	.433	70.6	3B	85	T-10 B-9	1.5 1	6 5	0 20	90	20-T UN-B			.5	MS	M
RC43-222H	402	.26	25.40	.871	500	.505	60.4	3	30										MS	M
RC46-047/073V	362	.09	7.10	.807	500	.362	63.3	3B	45	B-13	3	6	8	82	35-B	2	.5	.5	MS	M
RC44-073H	326	.09	5.90	.921	500	.377	86.2	3A	80	11	3	8	86	82	50			.5	MS	M
RC44-060H	227	.11	11.70	.639	500	.403	127.7	3	75	8	1	5	90	64	30				MS	M
RC46-083/110V	800	.62	37.70	1.068	500	.309	66.7	3A	90	9	2	7	4	86	35				MS	T
RC44-086H	390	.11	9.80	.999	500	.245	25.8	2A	100	8	1	6	85	90	55				MS	M
RC46-147/173V	271	.15	14.00	.846	500	.424	69.7	3	85	10	2	7	10	80	30				MS	M
RC44-156H	175	.06	5.50	.834	500	.794	54.0	3A	90	9	2	7	78	30	15				MS	M
RC46-246/272V	446	.09	9.30	1.006	500	.428	76.5	3A	90	2	10	7	8	82	40				MS	T
RC44-256H	271	.08	6.60	.818	500	.410	56.4	3B	70										MS	T
RC47-025/053V	322	.10	9.00	.782	500	.394	81.1	3A	80	T-10 B-10	3 3	9 6	0 0	90 90	55-T 80-B				MS	M
RC45-040H	306	.06	6.30	.671	500	.363	142.2	2A	90	11	2	6	80	30	70				MS	M-B
RC47-191/217V	669	.11	6.00	1.144	500	.244	50.2	3A	90	10	2	7	5	83	25				MS	M
RC44-204H	561	.16	16.60	1.074	500	.269	46.7	3A	90	9	3	5	85	80	30				MS	M-B
RC47-275/302V	326	.17	18.50	.815	500	.377	59.9	2A	100	T-15 B-7	3 3	8-T 5-B	20		UN				S	M
RC44-288H	366	.12	15.00	.854	500	.445	73.5	3B	50									.5	MS	M

FILE STR.UC.-2-20

SAMPLE #	01	02	03	04	05	06	07	08	09	10	11	12	13	14	15	16	17	18	19	20
RA01-009/036	597	.08	.12	.765	.12		182.4	1										3.0	S	T-M
RA01-078/105	1130	.13	.16	.887	.16		126.9	3	30										L	M-B
RA01-339/366	1361	.13	.16	1.068	.16		37.5	3B	50											
RA01-428/455	1476	.16	.17	1.024	.17		34.5	3B											S	M
RA06-058/085	971	.09	.13	1.522	.13		93.8	3										2.0	S	M
RA06-266/293	1194	.13	.15	.882	.15		121.3	3B					T-20	78	26-T	1	4.0	1.0	S	M
RC29-251/278	1448	.13	.16	1.232	.16		27.0	3	80	3	12	5							S	B
RC31-350/377	1058	.09	.13	1.156	.13		30.6	3	40	3	13	9							S	M
RC31-416/443	1520	.12	.18	1.255	.18		14.1	2A												

FILE STR.UC.-4-20

SAMPLE #	01	02	03	04	05	06	07	08	09	10	11	12	13	14	15	16	17	18	19	20
RC32-231/258V	963	.21	22.50	1.233	500	.504	46.2	2A		15	3	10	15	76	55					
RC43-245H	546	.08	9.50	1.159	500	.306	29.9	2A	100	12	3	7	86	12	50				MS	M-B
RC32-267/294V	661	.14	21.10	1.036	500	.253	42.1	2A	100	10	2	9	6	84	35				MS	M
RC33-268/295V	899	.14	13.50	1.278			24.0	2A	100	12	1	9	8	84	50				MS	M
RC43-280H	708	.11	9.70	1.490	500	.202	38.5	2A	100	18	2	10	90	5	30				MS	M
RC32-303/328V	573	.13	11.70	.878	500	.389	64.1	3B	40	5	2	5						.5	MS	M
RC43-316H	342	.07	8.20	1.191	500	.675	29.8	2A	100	9	4	7	85	25	30				MS	B
RC32-343/396V	485	.17	23.90	.776	500	.361	88.5	3	90	6	2	5							MS	M-B
RC43-357H	597	.14	14.40	.965	500	.400	58.7	3B	40			8				1	.5	1.0	MS	M
RC33-242/268V	947	.19	19.40	1.287			30.1	2A	100	14	2	8	10	82	60				MS	M
RC43-257H	541	.10	11.00	1.144	500	.397	24.4	2A	100	8	1	7	85	5	40				MS	M
RC33-368/395V	939	.18	14.20	1.101	500	.263	40.6	3	85	7	2	5						.5	MS	M
RC43-381H	867	.13	14.30	1.179	500	.239	31.0	3	75	5	2	4				2	.5	.5	MS	B
RC46-121/147V	517	.10	10.50	.101	500	.315	72.1	3B	50										MS	M-B
RC44-128H	255	.08	9.50	.952	500	.592	28.4	2A	100	10	2	7	65	24	50				MS	M
RC46-173/199V	493	.11	12.10	.873	500	.355	70.4	3B	40										MS	M-B
RC44-186H	1018	.13	12.40	1.292	500	.297	31.6	3A	95	10	2	8	0	90	30				MS	T
RC46-276/303V	629	.12	13.40	.952	500	.355	68.7	3B	40										MS	M
RC44-299H	609	.12	13.50	.900	500	.442	48.9	3B	30										MS	T-M
RC47-090/116V	1798	.19	20.70	1.311	25.70		41.0	2A	100	10	1	7	2	88	30				L	T-M
RC44-103H	505	.10	7.30	1.101	500	.386	34.8	2A	100	12	1	7	90	20	40				MS	M
RC44-116H	243	.07	6.60	.921	500	.457	25.3	2A	100	11	2	8	90	25	45				MS	M
RC47-127/153V	1846	.18	14.60	1.406	14.60		25.2	2A	95	10	3	7	2	88	40					
RC44-141H	287	.08	9.30	.896	500	.470	4.7	2A	100	11	3	8	90	35	30				MS	M
RC47-302/329V	875	.11	10.00	1.352	500	.282	15.0	3	75	8	3	5	90	0	15				MS	T-M

FILE STP.CC.-3-5/0.5

SAMPLE #	01	02	03	04	05	06	07	08	09	10	11	12	13	14	15	16	17	18	19	20
RA10-059/086	793	.28	2.80	.281	50.00	1.000	155.7	3	20			6	B-74	34	60-B	3	.5	1.0	MS	M-B
RA10-490/517	1630	.59	5.80	.310	50.00	.748	68.2	3B	30							3	.5	1.0	MS	T
RA11-233/260	1544	.44	4.20	.351	50.00	.634	86.7	3	50	9	2	7	20	72	60	4	1.0	1.0	MS	T-M
RB13-286/313	1870	.41	4.00	.456	50.00	.766	52.2	3B	60				40	80	100	3	.5	1.0	MS	M
RB16-124/151	1926	.52	4.70	.370	50.00	.508	85.3	2A	95	12	4	8	22	69	110				MS	M
RB16-262/289	1294	.35	3.10	.370	50.00	.554	108.9	3	75							T-B-10	2	1.0-T 5-B	MS	M
RB17-236/263	1838	.42	3.90	.438	50.00	.775	76.8	1								2	.5	1.0	MS	M
RB17-267/294	1584	.60	5.60	.264	50.00	.899	48.1	1								5	1.0	2.0	MS	M
RB17-399/426	2602	1.01	10.60	.258	50.00	.694	20.6	3B	20							2	.5	1.0	MS	M

FILE STR.CC.-5-5/0.25

SAMPLE #	01	02	03	04	05	06	07	08	09	10	11	12	13	14	15	16	17	18	19	20
RA08-134/161	460	.94	930		5000	.783	107.9	1								5	.5	1.0	MS	M
RA08-166/193	427	.79	750	.707	5000	.726	79.3	3	10			3				4	.5	1.0	MS	T-M
RA08-198/225	366	.92	940	.168	5000	.891	107.5	3	15			3				6	.5	1.0	MS	M
RA08-259/286	515	.58	590	.408	5000	.649	89.4	3	75	7	2	4	6	84	90	4	.5	1.0	MS	M-B
RA08-290/317	573	.79	820	.291	5000	.702	64.3	3	50	10	2	7	22	68	125	4	1.0	2.0	MS	M
RB12-077/104	166	.36	342	.217	5000	.994	60.6	2A	100			5	50	40	50				MS	T-M
RB12-163/190	555	1.00	999	.309	5000	.679	70.2	1								3	.5	1.0	MS	M
RB12-194/221	549	1.00	999	.245	5000	.685	65.3	1								3	.5	1.0	MS	M
RB13-066/093	286	.49	444	.179	5000	.804	67.7	2A	100	5	2	4	30		UN				MS	M
RB13-097/124	253	.39	390	.194	5000	.794	75.2	2A	100			5	50		UN				MS	M

FILE STR.CC.-5-5/0.5

FILE STR.CC.-5-5/0.5

SAMPLE #	01	02	03	04	05	06	07	08	09	10	11	12	13	14	15	16	17	18	19	20
RA10-236/263	>330	>5.00	>5000	.172			176.3	3	15			4				4	.5	1.0	MS	M-B
RA10-372/399	557	1.32	1340	.339	5000	.871	203.8	1								3	.5	1.0	MS	M
RA10-459/486	446	2.81	2810	.267	5000	.991	104.3	3B	20							4	.5	1.0	MS	M-B
RA10-536/563	895	.96	960	.297	5000	.716	32.3	3	65	7	2	4	12	78	55	3	.5	1.0	MS	T
RB13-255/282	362	.65	660	.212	5000	.967	62.3	3	80			6	60		UN	3	.5	1.0	MS	M
RB16-230/257	489	.73	730	.209	5000	.879	88.2	3B	40			3	52	60	60	2	.5	1.0	MS	M
RB16-330/357	350	.91	910	.362	5000	.943	58.0	3	60	7	2	5	80	23	25	2	.5	1.0	MS	M
RB17-367/394	577	.90	910	.287	5000	.910	27.9	3B	40				T-68	39	25-T	2	.5	1.0	MS	T-M
RB17-443/470	959	.52	540	.436	5000	.652	25.2	2A	90	T-4 8-8	1 2	3-T 7-8	12	78	30				MS	M-B

FILE STR.CC.-3-20/0.25

FILE STR.CC.-3-20/0.25

SAMPLE #	01	02	03	04	05	06	07	08	09	10	11	12	13	14	15	16	17	18	19	20
RA08-025/052	2125	.61	6.00	.482	50.00	.524	128.0	1								3	.5	1.0	MS	T
RA08-340/367	2467	.70	7.20	.334	50.00	.403	21.4	3B	50	9	1	5				7	1.0	2.0	MS	M
RA11-078/105	1679	.46	4.60	.428	4.60		112.7	3B	40	6	1	4	12	79	60	3	1.0	2.0	S	M
RA11-127/154	1822	.47	4.80	.470	50.00	.406	140.4	3B	40			6				2	.5	1.0	MS	M
RB12-132/159	2475	.65	6.40	.555	50.00	.431	84.8	1								4	1.0	2.0	MS	M
RB12-326/353	2157	.61	6.30	.297	50.00	.476	49.3	3B	20							5	.5	1.0	MS	M
RB12-047/074	1974	.61	6.10	.546	50.00	.399	73.9	2A	100			7	66	54	35				S	T-M
RB12-239/266	2236	.58	5.70	.589	50.00	.416	42.4	3B	60	9	2	6	90	70	20	4	1.0	2.0	MS	M-B
RB13-156/183	2332	.69	6.90	.536	50.00	.440	40.4	3B	50	9	3	7	65		UN	3	1.0	1.0	MS	T-M

FILE STR.CC.-3-20/0.5

SAMPLE #	01	02	03	04	05	06	07	08	09	10	11	12	13	14	15	16	17	18	19	20
RA10-194/221	2674	.61	5.40	.830	50.00	.700	98.4	3	10							4	.5	1.0	MS	M-B
RA10-341/368	2578	.79	7.80	.689	50.00	.760	103.5	3	10							2	.5	1.0	MS	M
RA10-567/594	4011	.88	8.50	1.021	50.00	.547	18.0	3	40	8	2	6	10	80	80	3	.5	1.0	MS	M
RB13-225/252	3008	.68	6.60	.901	50.00	.481	39.9	3	90	9	2	5	86	19	40			3.0	MS	M
RB13-342/369	4584	1.00	9.40	.936	50.00	.653	33.2	3	40	B-9	2	7	8		UN-B				MS	T
RB16-089/116	3374	.49	4.50	.838	4.50		85.0	3	15	5	2	3				4	.5	1.0	MS	M-B
RB16-392/419	3629	.91	9.00	.860	50.00	.544	22.6	3	50			4				3	.5	1.0	MS	M
RB17-052/079	1210	.21	2.00	.639	2.00		64.7	1								3	1.0	2.0	S	T&B
RB18-363/390	5602	1.20	12.00	1.000	50.00	.523	14.8	3	60			4	7	83	30	3	.5	1.0	MS	B

FILE STR.CC.-5-20/0.5

FILE STR.CC.-5-20/0.5

SAMPLE #	01	02	03	04	05	06	07	08	09	10	11	12	13	14	15	16	17	18	19	20
RA10-90/117	>740	>5.00	>5000	.303			123.5	3	25			4				4	.5	1.0	MS	M
RA10-133/160	851	1.52	1530	.479	5000	1.000	112.9	1								3	.5	1.0	MS	T-M
RA11-266/293	1039	.70	710	.297	5000	.743	95.9	3	75	12	2	8	64	30	30	3	.5	1.0	MS	M-B
RB16-156/183	>573	>5.00	>5000	.282			127.1	3A	70	8	3	6	35	67	90			1.0	MS	T-M
RB16-188/215	820	1.01	1030	.300	5000	1.000	99.0	3	20							7	.5	1.0	MS	M
RB16-361/388	971	.78	750	.318	5000	.836	33.9	3	80	T-8 B-6	2 2	4-T 3-B	66	26	70			2.0	MS	M-B
RB16-432/459	1600	.68	670	.452	5000	.592	21.7	2A	90	8	1	4	10		UN				S	T
RB17-191/218	963	1.39	1380	.386	5000	.975	77.1	3	10							4	.5	1.0	MS	T-M
RB17-335/362	1050	1.10	1110	.391	5000	.910	50.4	3B	60							3	.5	1.0	MS	M

FILE STR.UT.-3-5

SAMPLE #	01	02	03	04	05	06	07	08	09	10	11	12	13	14	15	16	17
RA03-073/100	115.0	.013	.32	.812	107.7	3B	25										B
RA07-149/176	116.0	.011	.33	1.124	93.4	2A	100	10 A-10 B-10	2 2 2	6 5-A 7-B	10	80	55				T
RA07-263/290	71.3	.008	.26	.943	81.9	3	40			6				5	1.0	2.0	T
RB14-232/259	76.0	.008	.26	.945	109.2	3B	80							5	2.0	4.0	T
RB14-263/290	120.0	.012	.33	1.054	60.9	3B	60			5				6	1.0	3.0	T
RB20-039/066	60.4	.007	.23	.977	118.8	3B	60	6	2	4							T
RB20-161/188	91.5	.009	.27	.931	65.5	3	25							9	1.0	3.0	B
RB20-193/220	84.2	.007	.25	1.207	57.0	3	95	12	2	7	10	80	50	3	1.0	2.0	B
RB221-005/032	69.6	.011	.27	.616	288.0	2A					70	36	80				B

FILE STR.UT.-5-5

SAMPLE #	01	02	03	04	05	06	07	08	09	10	11	12	13	14	15	16	17
RA07-181/208	135.0	.018	21.80	.913	77.6	38	25	7	2	5						2.0	B
RA09-036/063	149.0	.022	21.20	1.100	112.6	1								2	1.0	1.0	T
RA09-291/318	138.0	.019	28.60	1.020	24.7	3	70	A-7	2	5-A				7	1.0	3.0	B
RB20-129/156	94.6	.014	14.00	.990	80.5	3	85	10	3	6	52	38	60				T
RB21-164/191	113.0	.020	19.80	.889	64.2	38	75	11	3	6						4.0	T
RB21-196/223	82.1	.019	32.30	.887	56.5	3	90	10	2	4	30		UN			B-2.0-B	M
RB21-257/284	136.0	.019	25.30	.817	70.2	3	10							6	.5	1.0	T
RB22-018/045	94.6	.021	24.90	.786	139.1	3	70			6	70	20	40				M
RB22-163/190	130.0	.081	17.00	.940	78.1	3	30	9	2	6	20		UN	A-2	.5	1.0-A	B

FILE STR.UT.-3-20

SAMPLE #	01	02	03	04	05	06	07	08	09	10	11	12	13	14	15	16	17
RA03-042/069	123.0	.012	.31	1.039	98.2	38	30										B
RA03-127/154	121.0	.012	.32	.967	102.6	38	15							4	.5	1.0	B
RA09-234/261	69.0	.009	.28	.955	88.8	3								5	1.0	3.0	B
RB14-025/052	84.2	.009	.16	1.003	129.9	3	25							10	2.0	5.0	B
RB14-294/321	133.0	.012	.31	1.177	44.0	38	60			6				3	.5	1.0	B
RB20-089/116	134.0	.012	.32	1.158	64.2	3	75	B-13	3	6-B	8		UN			2.0	T
RB20-262/289	92.5	.009	.27	1.117	50.0	3	20	8	3	4				5	.5	2.0	T
RB21-361/388	124.0	.012	.32	1.072	56.1	3								5	1.0	3.0	B
RB22-132/159	104.0	.010	.31	1.048	57.9	1								4	.5	1.0	T

FILE STR.UT.-5-20

FILE STR.UT.-5-20

SAMPLE #	01	02	03	04	05	06	07	08	09	10	11	12	13	14	15	16	17
RA03-192/219	93.5	.010	9.80	1.134	65.9	3	10							9	.5	1.0	B
RA03-243/270	123.0	.014	14.10	1.011	94.3	38	30			6				5	1.0	2.0	M
RA03-341/368	126.0	.014	15.50	1.069	40.0	3	40							4	1.0	2.0	B
RA07-005/032	78.0	.014	14.60	.604	200.1	3	10			4						2.0	T
RA09-129/156	92.5	.011	12.10	.967	82.6	3	80			6	56	34	50			1.0	B
RA09-160/187	89.4	.012	12.30	.788	104.8	3								4	1.0	3.0	M
RB14-185/212	71.4	.009	10.60	.919	74.8	1											T
RB14-368/395	134.0	.022	24.50	1.039	28.8	2A	100	17	3	7	76		UN				
RB20-231/258	124.0	.012	15.80	1.006	45.6	3B	25			4				4	1.0	2.0	B